Miniaturized therapeutic systems for ultrasound-modulated drug delivery to the central and peripheral nervous system

Zhu, Pancheng; Simon, Ignasi; Kokalari, Ida; Kohane, Daniel S.; Rwei, Alina Y.

DOI
10.1016/j.addr.2024.115275

Publication date
2024

Document Version
Final published version

Published in
Advanced Drug Delivery Reviews

Advanced Drug Delivery Reviews 208 (2024) 115275

Contents lists available at ScienceDirect

Advanced Drug Delivery Reviews

journal homepage: www.elsevier.com/locate/adr

Miniaturized therapeutic systems for ultrasound-modulated drug delivery to the central and peripheral nervous system

Pancheng Zhu [a,b,c,1], Ignasi Simon [a,1], Ida Kokalari [a], Daniel S. Kohane [d,*], Alina Y. Rwei [a,*]

[a] Department of Chemical Engineering, Delft University of Technology, 2629 HZ, Delft, the Netherlands
[b] State Key Laboratory of Mechanics and Control of Aerospace Structures, Nanjing University of Aeronautics & Astronautics, 210016, Nanjing, China
[c] Department of Biomedical Engineering, The Hong Kong Polytechnic University, Hong Kong, China
[d] Laboratory for Biomaterials and Drug Delivery, Department of Anesthesiology, Boston Children's Hospital, Harvard Medical School, Boston, MA 02115, USA

GRAPHICAL ABSTRACT

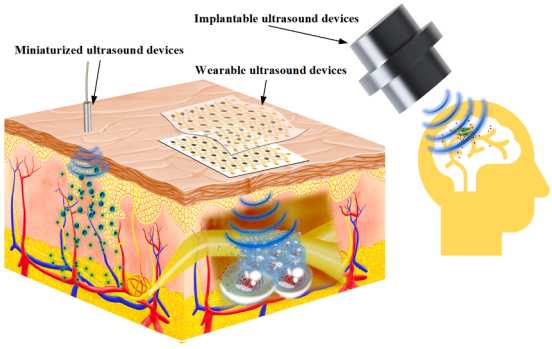

ARTICLE INFO

Keywords:
Cavitation
Microbubble
Sonochemistry
Sonosensitizer
Wearable device
Implantable device
Ultrasound transducer

ABSTRACT

Ultrasound is a promising technology to address challenges in drug delivery, including limited drug penetration across physiological barriers and ineffective targeting. Here we provide an overview of the significant advances made in recent years in overcoming technical and pharmacological barriers using ultrasound-assisted drug delivery to the central and peripheral nervous system. We commence by exploring the fundamental principles of ultrasound physics and its interaction with tissue. The mechanisms of ultrasonic-enhanced drug delivery are examined, as well as the relevant tissue barriers. We highlight drug transport through such tissue barriers utilizing insonation alone, in combination with ultrasound contrast agents (e.g., microbubbles), and through innovative particulate drug delivery systems. Furthermore, we review advances in systems and devices for providing therapeutic ultrasound, as their practicality and accessibility are crucial for clinical application.

* Corresponding authors.
E-mail addresses: Daniel.Kohane@childrens.harvard.edu (D.S. Kohane), A.Y.Rwei@tudelft.nl (A.Y. Rwei).
[1] These authors contributed equally to this work.

https://doi.org/10.1016/j.addr.2024.115275
Received 12 December 2023; Received in revised form 19 February 2024; Accepted 1 March 2024
Available online 3 March 2024

1. Introduction

Ultrasound is an energy source that can be used for a myriad of medical treatments, due to its ability to effectively penetrate tissue and produce non-invasive biological therapeutic effects [1]. Beyond its established applications in physical therapy, ultrasound emerges as a promising technology to overcome some current limitations of drug delivery, such as restricted drug penetration of biological barriers and ineffective targeting. Indeed, ultrasound application has demonstrated refined spatial targeting and enhanced drug penetration through biological barriers such as the blood–brain barrier (BBB) [2].

Effective therapeutic delivery to the nervous system is crucial for the treatment of neuropathological diseases that impose significant challenges in current health care, including pain, dementia, and epilepsy. In the central nervous system (the brain and spinal cord) the BBB and blood-spinal-cord barrier (BSCB) are the main tissue barriers for systemic (i.e., through the bloodstream) drug delivery [3]. The peripheral nervous system consists of nerves branching out from the central nervous system, with the blood-nerve barrier being the main barrier to systemic drug delivery and the perineurium being the main barrier to delivery from surrounding tissues [4]. Various physico-chemical and pharmacological methods have been explored to bypass the associated tissue barriers and enhance drug delivery to the central and peripheral nervous systems [2]. These methods include chemical modification of drugs to alter lipophilicity and facilitate their passage through the lipid-rich tissue barriers, encapsulation of drugs in drug delivery systems to improve flux into the nervous system, co-administration of hyperosmotic solutions to increase permeability of tissue barriers, direct transcranial injection via catheters, and intranasal administration [5]. However, many of these methods suffer from insufficient drug delivery to the target area or are invasive approaches.

Recently, ultrasound, alone or in combination with particle-based systems, has demonstrated promising clinical applications for drug delivery to the nervous system [6]. Ultrasound-mediated techniques leverage thermal, mechanical, and/or sonochemical effects to provide spatiotemporal control. Conventional ultrasound devices are bulky instruments with stiff interfaces. Recently, technological advances have led to miniaturization of ultrasound equipment with mechanical properties matching the target tissue. Miniaturized ultrasound-generating devices have been utilized in applications such as in situ imaging [7], neuromodulation [8], and drug delivery [9]. A range of biocompatible flexible and implantable ultrasound devices have evolved to enable ultrasound-modulated spatiotemporal control of therapeutic events upon direct contact with the nervous tissue [10].

Successful clinical integration of advanced ultrasound-based therapeutic systems relies on the development of both the drug delivery system and the ultrasound generating system, as they are coupled in therapeutic use. This review therefore focuses on the recent advances in both the drug delivery system for ultrasound-triggered drug release to the central and peripheral nervous system and advances in ultrasound-generating devices that could enhance therapeutic outcomes and the patient experience. We commence by exploring the fundamental principles of ultrasound physics and its interaction with tissue. The mechanisms of ultrasonic-enhanced drug delivery are examined, as well as the relevant tissue barriers that hinder the delivery of nervous system-targeted drugs. We highlight drug transport through such tissue barriers utilizing insonation alone, in combination with ultrasound contrast agents (e.g., microbubbles), and by particulate drug delivery systems. We review recent advances in systems and devices for providing therapeutic ultrasound, that may facilitate clinical application. Finally, we discuss the major challenges of developing ultrasound-modulated therapeutic systems and provide a critical perspective on the future of this evolving field.

2. Physics of ultrasound and interaction with tissue

2.1. Definitions in ultrasound physics

Sound is a mechanical wave, which causes mechanical disturbance in the medium and transfers mechanical energy from one point to another. When sound waves pass through a medium, energy propagates through the collisions of adjacent particles, which oscillate near their stationary positions with no net displacement [11].

Sound waves can be longitudinal or transverse, depending on their oscillation direction relative to the direction of energy passing through the medium. Only elastic solids can propagate sound waves transversely, while all materials can support longitudinal waves. When traveling through soft tissues and fluids within the body, longitudinal waves are dominant [12].

The frequency of a sound wave (in hertz, Hz) is the number of oscillations (or cycles) per second. If the particle completes a complete oscillation once per second, its frequency is 1 Hz. Ultrasound is a form of sound wave, with a frequency higher than the upper limit of human hearing, typically exceeding 20 kHz [11,12]. Ultrasound tissue penetration depth is highly dependent on its frequency, as detailed in *Section 2.2*.

Acoustic pressure is a scalar quantity used to indicate the amplitude of sound at a specific location. It is the deviation from the ambient atmospheric pressure caused by a sound wave. The SI unit for acoustic pressure is the Pascal (Pa) [13]. Intensity is a measure of energy in a sound beam, a key characteristic to determine the potential of tissue damage upon insonation. It is often expressed in power per area, e.g., watts per square meter. The relationship between acoustic pressure and intensity is as follows (Eqn (1):

$$p = \sqrt{2I \bullet Z} \tag{1}$$

where p is the sound pressure (Pa), I is the intensity (W/m^2), and Z is the acoustic impedance ($Pa{\cdot}s{\cdot}m^{-1}$) [14].

During sonication, energy input is interlinked with two key variables: mechanical index and thermal index [15]. The mechanical index (MI) represents the probability of cavitation. It is the peak negative pressure (in MPa) divided by the square root of the ultrasound frequency (in MHz). The FDA recommends a maximum MI of 1.9 for diagnostic ultrasound devices to ensure safety [16]. The thermal index (TI) is related to the increase in tissue temperature. TI is defined as the attenuated acoustic power at the tissue depth of interest, divided by the power necessary to raise the tissue temperature by one degree Celsius. A $TI < 2$ (corresponding to an approximate 4 °C temperature increase in soft tissue) is recommended by the American Institute of Ultrasound in Medicine (AIUM) for ultrasound exposure up to 15 min [16].

2.2. Ultrasound interaction with biological tissue

Ultrasound can generate a wide range of biological effects through its interaction with tissue [17]. Understanding the physical interactions between ultrasound and tissue provides a scientific basis for the design and risk assessment of ultrasound in therapeutic applications [18].

Ultrasound attenuation is the reduction in intensity or amplitude of the waves as they propagate through a medium and is quantified in decibels per centimeter of tissue traversed per megahertz (dB/cm/MHz). Attenuation is quantified by the attenuation coefficient (α_t), which is expressed in (dB/cm/MHz). For the majority of tissues, attenuation values typically fall within the range of 0.3–0.8 dB/cm/MHz, as detailed in Table 1 [19]. Attenuation is dependent on the frequency of the ultrasonic beam (f) and the distance traveled by the beam (z) (Eqn (2) [20].

$$\alpha_t = 10 \times z^{-1} \times f^{-1} \times log_{10}(I/I_t) \tag{2}$$

where I_t is the transmitted acoustic intensity and I is the input acoustic

Table 1
Attenuation coefficient of various tissues [19].

Tissue/ Medium	Attenuation coefficient (dB/ cm/MHz)*	Acoustic impedance ($MPa \cdot s \cdot m^{-1}$)
Water	0.0022	1.5
Blood	0.15	1.6
Soft tissue	0.75	1.6
Air	7.50	0.00001
Bone	15.0	8.0
Fat	0.63	1.4
Kidney	1.0	1.6
Lens of eye	0.05	1.7

*The unit of the attenuation coefficient is decibels per centimeter of tissue traversed per megahertz.

intensity.

When the ultrasound beam passes through a uniform tissue, its energy is attenuated through reflection, refraction, scattering and absorption (Fig. 1), detailed as follows[21,22]:

- Reflection: when ultrasound waves encounter a boundary between two tissues with different acoustic impedance (the product of the tissue density and the speed of sound in the tissue), a portion of the wave is reflected. The amount of reflection depends on the impedance mismatch between the tissues.
- Refraction: wave refraction is the bending of a wave as it passes through from one material to another. When waves hit a surface of a different medium, some waves are reflected, while the rest bend and change direction. The fraction refracted is quantified by the refraction coefficient.
- Scattering: when ultrasound encounters small structures or variations in tissue density, such as cell boundaries or tissue interfaces, it scatters in various directions.
- Absorption: the mechanical energy of ultrasound can be absorbed by tissue and converted into heat.

Thus, attenuation increases with frequency, so lower frequencies are often used to penetrate deeper into the tissue. Most importantly, unlike light waves, ultrasound is less absorbed by water and tissues, resulting in greater penetration depths [23]. Penetration depth characterizes the distance an energy source penetrates through a given medium; its standardized definition is the depth at which the intensity of the radiation inside the material falls to 1/e (about 37 %) of its original value at the surface [24]. When compared to other external energy sources, such as light, ultrasound has longer wavelengths and lower energy, inducing less tissue scattering and absorption in biological tissues, achieving a penetration depth of 3–5 cm at a frequency of 1 MHz, compared with $<$ 1 mm for visible light and $\sim$ 1 cm for near-infrared light [25]. Therefore, ultrasound can be used for deep tissue imaging, as evidenced by the clinical use of diagnostic ultrasound, and can be used to transmit energy into the body at precise locations, which is key to therapeutic applications. Safe, non-invasive, and painless energy transmission into the body is crucial for ultrasound-activated drug delivery.

3. Mechanisms of ultrasound-mediated drug delivery

Ultrasound-generated effects can be categorized into thermal, mechanical, and sonochemical. Thermal effects are generated through the absorption of ultrasound energy by tissues and drug-delivery materials. Mechanical effects, such as cavitation and acoustic streaming, are the main working mechanisms for microbubble-based drug delivery systems [26]. Sonochemical effects make use of the ultrasound harvesting properties of molecules such as sonosensitizers [27]. This section will discuss the mechanism of these ultrasound-generated effects, focusing on their interactions with biological tissue and applications in drug delivery systems.

3.1. Thermal effects

The conventional use of therapeutic ultrasound is tissue heating. Raising the temperature to a few degrees above the normal body temperature level may induce beneficial physiological effects, such as increasing local tissue perfusion [28]. The ultrasound energy absorbed by tissue is converted into thermal energy, heating the exposed tissue. This thermal effect increases with ultrasound frequency and is most significant at the MHz range. Numerous preclinical studies have shown that the release of therapeutic drugs encapsulated in temperature-sensitive liposomes (TSLs) under hyperthermic conditions generated by ultrasound can significantly improve the concentration, distribution, and ultimate therapeutic effect of the given dose [29,30]. When the temperature reaches the melting phase transition temperature of the lipid bilayer, the structure of the lipid membrane changes from the gel phase to liquid crystal phase, and TSL releases the encapsulated drug [31]. In cancer therapy applications, ultrasound-induced hyperthermia in combination with TSL induces tumor ablation and achieves spatio-temporal control of chemotherapeutic release with TSL [32]. Liver tumor patients were treated with a single intravenous infusion of chemotherapeutic-loaded (i.e., doxorubicin) TSL during a phase 1 clinical trial, followed by extracorporeal focused ultrasound insonation at their liver tumor. An average increase of 3.7 times in intratumoral chemotherapeutic concentration [33] was found via biopsy, demonstrating enhanced intratumoral drug delivery enabled through

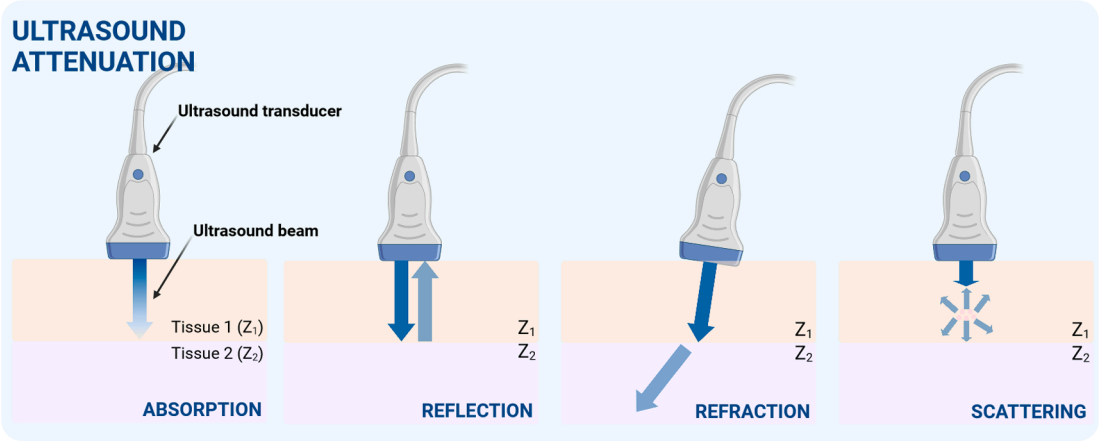

Fig. 1. Ultrasound attenuation mechanism when traveling through tissue. Z_1 and Z_2 indicate distinct acoustic impedances (Z) of tissue 1 and 2. The shading of the ultrasound beam relates to its acoustic intensity (e.g., a darker color indicates higher intensity). Illustrations were created with Biorender.com.

ultrasound-mediation.

Prolonged exposure to significantly elevated temperatures may have adverse effects on underlying tissues, including burns, necrosis (i.e., direct cell death), and adverse immune response [29]. The phase 1 clinical study with TSL mentioned above found that adverse immune events were triggered in half of the subjects. To minimize undesirable thermal effects, the temperature can be controlled by operating the ultrasound instrument in pulse mode, minimizing insonation intensity and duration. A tissue temperature of approximately 42° C induces beneficial biological effects (e.g., enhancement in blood circulation), while above this temperature tissue damage can occur in the form of DNA repair inhibition, direct cell death, and undesired immune response [34,35].

3.2. Mechanical effects

The mechanical effects from insonation can be classified into three categories: cavitation, acoustic streaming, and radiation forces.

3.2.1. Cavitation

Cavitation refers to the process of producing bubbles in a fluid when it is subjected to forces exceeding its tensile strength. Ultrasonic waves propagate in fluids and generate cavitation bubbles when the peak negative pressure has a large amplitude (above the tissue- and frequency-dependent cavitation threshold [36]). As a result of oscillating pressure waves, bubbles oscillate and grow during the progressing cycles of the pressure wave. Stable cavitation is the periodic growth and shrinkage of bubbles, oscillating near an average size; while inertial cavitation is the unstable growth and collapse of cavitation bubbles [37]. Ultrasound intensity, frequency, and the presence of ultrasound contrast agents are key factors in determining the mode of cavitation. An intensity above a tissue-dependent threshold is required for inertial cavitation. Beyond this threshold, the likelihood of inertial cavitation increases linearly with ultrasound intensity. The presence of exogenous ultrasound contrast agents (e.g., microbubbles) has been found to lower the cavitation threshold 2–3 fold [38], thereby inducing cavitation at lower ultrasound pressures. Frequency is also a key factor: inertial cavitation activity rapidly decreases with increasing ultrasound frequency at any given intensity [36,39]. Furthermore, the threshold intensity of inertial cavitation increases with ultrasonic frequency. This dependence reflects the fact that the growth of cavitation bubbles becomes increasingly difficult with increasing ultrasound frequency.

Insonation parameters can influence the size of the ultrasound-nucleated cavitation bubbles, which plays a significant role in ultrasound's therapeutic and safety profile. The size of the nucleated bubbles is inversely proportional to the ultrasonic frequency [40,41]. This provides further insights when understanding the mechanism of tissue damage from ultrasound exposure. For example, small bubbles generated by high ultrasound frequencies (with a radius of ~ 3 μm at 1 MHz) can nucleate within the voids of the stratum corneum (SC), promoting its ability to damage the ordered SC structure. In contrast, cavitation bubbles larger than the voids in SC are unlikely to enhance the permeation of the skin tissue barrier [42].

Ultrasound may mechanically disturb biological barriers and promote the transport of drugs to the target site through cavitation. The implosion of bubbles due to inertial cavitation generates microjets that create small pores within cell membranes, a process termed sonoporation [9]. The generated pores may be temporary (contributing to successful treatment delivery) or permanent (leading to tissue injury) [43]. Sonoporation has been found to enhance tissue barrier (e.g., skin) permeability [44].

Ultrasound can mechanically disrupt drug carriers through inertial cavitation. The shock waves generated by inertial cavitation induce jets of dense fluid passing through a vesicle, generating shear stress on the surface of a vesicle, which can shear or potentially puncture nearby vesicles. Drug-loaded liposomes, conjugated or co-administered with microbubbles, experience mechanical disruption and release their drug content upon insonation, demonstrated *in vivo* [45–48]. The aforementioned ultrasound-triggered drug release from the liposomes may be linked with the shear stress generated by the inertia cavitation of microbubbles.

3.2.2. Acoustic streaming

When a strong ultrasonic beam is directed through a liquid, momentum from the beam is transferred to the fluid, imparting a large-scale convective motion to the fluid that can also increase the overall rate of drug transport [49]. This is termed acoustic streaming, i.e. flow generated by the propagation of ultrasound in a fluid medium, and is the dominant convection effect generated by ultrasound. An example of its importance in drug delivery is seen in enhanced drug penetration through the gastric mucosa induced by mucosal compression and extension due to acoustic streaming under low power density insonation [50], Moreover, acoustic streaming induces the movement of materials (*e.g.* drugs) in a single direction (i.e., the direction of wave propagation) in tissues [51,52]. This directional bias is in contrast to temperature-dependent diffusion in which molecular movement occurs in all directions. In the study of articular cartilage exposed to focused ultrasound, the injected drug demonstrated a net maximum displacement of approximately 0.7 mm in the direction of wave propagation [53]. Acoustic streaming has also been proposed to promote angiogenesis [54], enhance tissue repair [55], and stimulate the hypothalamic area [56].

3.2.3. Acoustic radiation forces

Acoustic radiation forces are produced by the interaction of sound waves with obstacles in their path. When a gas bubble in a liquid is exposed to an acoustic pressure field, it can experience volume pulsations. Acoustic pressure gradients interact with the oscillating bubbles to create a translational force on the bubble, known as the primary Bjerknes force [57]. The resonant frequency of a bubble increases with decreasing bubble size [57]. Small bubbles with a resonant frequency greater than the driving frequency of the sound field move up a pressure gradient, while larger bubbles move down the gradient [58]. Such primary acoustic radiation forces produced by ultrasound bring microbubbles into contact with the vascular wall, which has been used to enhance drug penetration through tissue barriers [59].

Conversely, when cavitation bubbles oscillate in an acoustic field, the pressure field generated by their oscillation can lead to the mutual attraction or repulsion between the cavitation bubbles, a phenomenon known as the secondary Bjerknes force [60]. This interaction can drive bubble agglomeration, which may be utilized to enhance the ultrasound-triggered drug release events (see details in *Section 5.3.1*). In summary, primary and secondary Bjerknes forces (often referred to as primary and secondary radiation forces), play a significant role in the acoustic manipulation of particles. Comprehending these forces is important for designing and optimizing ultrasound-based applications across various domains [61].

3.3. Sonochemical effects

Sonochemistry refers to the use of ultrasound to drive chemical reactions. Sonodynamic therapy (SDT) relies on the interaction between ultrasound and sonosensitizers, in a manner analogous to the use of light and photosensitizers in photodynamic therapy (PDT). Under US irradiation, excitation of sonosensitizers from the ground to an excited state occurs, which leads to the generation of short-lived reactive oxygen species (ROS). The resulting oxidative stress can be exploited for targeted drug release and promote localized cell death for cancer treatment. However, the exact mechanism by which sonosensitizers produce ROS upon US irradiation is not fully elucidated. It is generally accepted that cavitation leads to the generation of ROS through cavitation-induced sonoluminescence or pyrolysis [62]. The rapid collapse of

bubbles during cavitation emits light, a process termed sonoluminescence [63]. Sonoluminescence subsequently excites the photoactive sonosensitizer to its excited state, generating ROS [64,65]. Localized rises in pressure and temperature can result in pyrolysis, exciting the sonosensitizer to generate ROS [66].

3.3.1. Sonosensitizers

Sonosensitizers are essential constituents for SDT therapy, as SDT efficacy is greatly dependent on the sonosensitizer's efficiency. Singlet oxygen quantum yield (Φ_Δ), a term commonly used for PDT, provides an important quantitative measurement of ROS generation for dosimetry. It refers to the efficiency with which a particular substance generates singlet oxygen molecules. It is a measure of the ratio of the number of singlet oxygen molecules produced to the number of absorbed photons. A higher Φ_Δ indicates more efficient ROS generation in response to light or ultrasound stimuli [67,68]. However, additional factors such as stability and cytotoxicity should also be considered in the selection of sonosensitizers.

The most extensively investigated sonosensitizers are organic porphyrin derivatives, including protoporphyrin IX (PPIX), hematoporphyrin monomethyl ether (HMME), hematoporphyrin (HP), and sinoporphyrin sodium (DVDMS). These molecules exhibit biocompatibility and possess both photosensitizing and sonosensitizing properties. Their sono/photosensitivity originates from their aromatic macrocyclic structure, characterized by the presence of highly delocalized conjugated systems that facilitate p-p* excitation under illumination or insonation, ultimately resulting in ROS generation [69]. Aggregation of porphyrin-based sonosensitizers impedes energy transfer between porphyrin and O_2, significantly reducing Φ_Δ . To circumvent such limitations, hemoglobin (Hb) has been proposed as both sonosensitizer and oxygen-carrying molecule [70]. Multidrug-resistant bacteria were targeted using a nanoparticulate system that loaded the sonosensitizer HMME into zeolitic imidazolate framework-8 (ZIF-8). The incorporation of Hb aimed to increase oxygen concentration in the hypoxic microenvironment of bacterial infection, thereby facilitating ROS generation upon insonation of the sonosensitizer [71]. In addition to porphyrins, other types of organic sonosensitizers include xanthenes, phthalocyanines, and indocyanines. The readers are referred to [72] for an in-depth discussion of advances in organic sonosensitizers.

Increasing interest has been given to inorganic sonosensitizers [73]. They offer enhanced stability under ultrasound and can be easily functionalized. However, the challenges of inorganic sonosensitizers include low ROS quantum yield, limited biocompatibility, and cytotoxicity, which hinder their therapeutic applications.

4. Tissue barriers

A major advantage of ultrasound is its ability to mechanically disturb tissue barriers to promote the flux of drugs into the nervous system. In this section, we discuss the major tissue barriers for drug delivery to the nervous system, providing context for discussions of ultrasound-enhanced drug delivery in *Section 5*.

4.1. The blood–brain barrier (BBB)

A major hurdle for systemically administered medications targeting the brain is navigating through the BBB [3]. The presence of tight junctions (TJs) and adherens junctions (AJs) between neighboring endothelial cells in the BBB creates a physical, transport, immunological, and metabolic barrier that isolate the CNS from systemic circulation, making the entrance of nutrients highly selective and hindering the passage of pathogens, toxins, and drugs [74]. Paracellular transport is prevented by TJs filling the paracellular space. Compounds primarily gain access to the brain through a combination of active transport, passive diffusion, and specific transporters such as GLUT1, insulin, and transferrin receptors. The BBB is highly impermeable to most molecules, especially polar hydrophilic and high molecular weight ones, thereby impeding drug delivery to the brain [75].

4.2. The nerve-tissue barrier and the blood-nerve barrier (BNB)

The peripheral nervous system is protected from its surrounding environment by three main barriers: the epineurium, the perineurium, and the endoneurium [4]. The epineurium is a connective tissue that surrounds the entire nerve. Its primary role is to provide mechanical support and maintain structural integrity. The perineurium is a dense connective tissue that encloses individual nerve fascicles. It controls the flux of interstitial fluid to cells within, maintaining homeostasis. As it is a main diffusion barrier for drug delivery to the target peripheral neurons, the perineurium is also termed the Nerve-Tissue Barrier. This Nerve-Tissue Barrier is formed by basal membranes and concentric layers of peripheral cells that are joined by tight junctions [76]. During local administration of drugs (e.g., local anesthetics) at the peripheral nerve, the perineurium is the main diffusion barrier [77]. The perineurial barrier impedes the access of hydrophilic drugs to their target neurons, limiting their effectiveness [78]. The endoneurium is a connective tissue sheath around individual myelinated axons[4].

The main barrier for systemically administered drugs to reach the target peripheral neuron is the blood-nerve barrier (BNB) [4,76]. It is located within the blood vessel wall of the endoneurial vasculature and forms tight junctions between endothelial cells and pericytes to maintain endoneurial homeostasis. Similar to the BBB, the BNB tightly restricts the passage of substances from the blood into the nerve environment. It exhibits low permeability to solutes and macromolecules, impeding systemic drug delivery to the peripheral nerve.

4.3. The skin barrier

Therapeutic agents can also be delivered through the skin via topical applications, such as topical application of local anesthetics for cutaneous pain relief [79]. The stratum corneum is the main diffusion barrier for such transdermal drug delivery. The stratum corneum is the outer layer of the epidermis, composed of structured corneocytes and lipids [80]. Each corneocyte possesses a highly cross-linked cornified envelope filled with keratin filaments. The individual corneocytes are surrounded by an extracellular lipid matrix, organized in a brick(corneocyte)-and-mortar (lipid matrix) structure. The human stratum corneum typically contains 20 corneocyte cell layers. This hydrophobic stratum corneum prevents the loss of water and other body constituents from the body. It also is the major diffusion barrier for topical drug delivery. Once this barrier has been overcome, drugs and drug delivery systems would have to overcome barriers to delivery to nerves within.

4.4. The cell membrane

The cell membrane regulates the movement of molecules between the cytoplasm and the extracellular space. It is composed of 50 % protein, 45 % lipid and 5 % carbohydrate [81]. It is relatively permeable to small hydrophobic molecules, while transport proteins and ion channels control the transport of hydrophilic solutes. Nanoparticles and macroparticles gain access to the cytosol via endocytosis and are translocated to intracellular vesicles including endosomes and lysosomes. The acidic pH and enzymes within such vesicles often degrade the endocytosed content, thereby imposing a barrier for drug delivery [82]. Ultrasound-mediated cavitation with the presence of microbubbles has been found to temporarily perforate the cell membrane, a process termed sonoporation [83]. Sonoporation enhances the delivery efficiency of drugs to the target cell, from small molecules [84] to macromolecules (e.g., antibodies [85] and genes [86]).

5. Ultrasound-mediated drug delivery

Ultrasound enhances the therapeutic effectiveness of pharmaceutics due to its ability to mechanically disturb tissue barriers, enhancing the ability of drugs to reach their target site (see *Section 5.1*). This effect can be further enhanced by co-application of microbubbles (see *Section 5.2*). Furthermore, materials used in drug delivery systems, such as lipids and polymers, have recently been designed to be responsive to the effects of ultrasound, so that drugs can be released in a region of interest at the desired time and dosage (see *Section 5.3*). A summary of ultrasound-modulated drug delivery in different tissues *in vivo* is presented in Table 2. This section discusses these advances in the application of ultrasound for enhanced drug delivery, focusing on the central and peripheral nervous system.

5.1. Drug transport enhanced by ultrasound alone

The mechanical effect of ultrasound drives convection processes that enhance drug transport through tissue [108]. For example, ultrasound has been used clinically to enhance the anesthetic effect of topical lidocaine [93]. Ultrasound exposure at 0.17 W/cm^2, 48 kHz, 100 % duty cycle on mice with feet immersed in local anesthetic aqueous solution showed significant anesthetic effect for 2 h, while the control group without ultrasound exposure showed no anesthetic effect [109]. The temperature rise of the solution was less than 1 °C. These results suggest that ultrasound-mediated mechanical effects may have been the predominant mechanism of the enhanced therapeutic efficacy.

Ultrasound can enhance the penetration of hydrophilic drugs through tissue barriers. Insonation enhanced therapeutic effectiveness from the hydrophilic local anesthetic tetrodotoxin injected at (outside) the sciatic nerve. Here, the therapeutic effect was measured as the duration and degree of nerve block (i.e., neurobehavioral effect due to the inhibition of nerve signal transmission by the peripheral nerve). Using a rat model and an ultrasound frequency of 1 MHz, the authors found that insonation at ultrasound intensities greater than 0.5 W/cm^2 resulted in a greater duration of nerve block than without insonation (at 3 W/cm^2, 4.6-fold longer), and greater flux of a fluorophore into the sciatic nerve (3-fold increase with 3 W/cm^2 insonation). While the exact mechanism for this effect is unclear, the authors suggested that both ultrasound-mediated thermal and mechanical effects may have played a role. The authors also observed that systemic distribution from the site of injection was enhanced by insonation. Interestingly, insonation did not affect nerve block from the local anesthetic bupivacaine, which is more hydrophobic than tetrodotoxin. This suggests that the effect of insonation on local anesthesia effectiveness depends on the hydrophilicity of the drug molecule; more hydrophilic molecules, which have more difficulty crossing biological barriers, would be helped more than more hydrophobic molecules.

Focused ultrasound was applied to patients with Alzheimer's disease upon coadministration of antiamyloid antibodies to enhance the delivery of the antibodies to the brain [100]. Patients were administered antiamyloid antibodies intravenously monthly. Two hours after each administration focus ultrasound was applied. The opening of the blood–brain barrier was visualized by gadolinium contrast MRI. After 26-weeks of treatment, a 48 %-63 % reduction in amyloid-beta levels was detected by fluorine-18 florbetaben positron-emission tomography. Adverse events including headaches and hypertension resolved 180 days after the last insonation event.

5.2. Ultrasound-enhanced drug transport with ultrasound contrast agents

Ultrasound contrast agents, such as microbubbles and phase change perfluorocarbon nanodroplets, have the ability to amplify the mechanical effects of ultrasound [110]. Microbubbles are micron-scale gas particles stabilized by surfactants (e.g., lipids or proteins [111,112]). Phase change perfluorocarbon nanodroplets are liquid-filled submicron particles, commonly formed by the condensation of microbubbles, and vaporize upon insonation to form microbubbles in situ [113]. Upon insonation, the microbubbles undergo high-frequency vibrations alternating between expansion during peak negative pressures and contraction during peak positive pressures. These vibrations exert forces on adjacent cells, inducing the disturbance of cell barriers.

Microbubble-facilitated low-intensity pulsed ultrasound (LIPUS-MB) can temporarily disrupt the BBB in various animal models, enhancing

Table 2
A representative summary of ultrasound-mediated drug delivery systems in different tissues.

Tissue	Animal model	Drug delivery system	Ultrasound contrast agent	Mechanism of ultrasound mediation	Reference
Skin	Rat	Free drug	Microbubble	Mechanical	[87]
		Hydrogel	None		[88]
			Nanobubble		[89]
		Inorganic nanoparticle	None	Thermal	[90]
		Free drug		Thermal & Mechanical	[91]
	Pig	Free drug		Mechanical	[92]
	Human	Free drug		Thermal & Mechanical	[93]
Subcutaneous tumor	Rat	Free drug		Sonochemical	[27]
		Liposome			[68]
		Hydrogel		Mechanical	[94]
		Polymersome			[95]
		Nanobubble	Nanobubble		[96]
		Free drug	Microbubble		[97]
Brain	Rat	Liposome			[48]
	Rabbit	Free drug			[98]
	Human	Free drug			[99]
			None		[100]
Sciatic nerve	Rat	Liposome	None	Sonochemical	[101]
		Free drug		Thermal & Mechanical	[102]
		Polymeric microparticle		Mechanical	[103]
		Hydrogel	Microbubble		[104]
Cartilage	Rat	Liposome	None	Sonochemical	[105]
Gastrointestinal tract	Pig	Free drug		Mechanical	[106]
Hind leg tumor	Rat	Liposome	Microbubble		[45]
Immune system*	Rat	Polymeric nanoparticle			[107]
Kidney	Rabbit	Liposome			[46]
Liver	Human	Liposome	None	Thermal	[33]

*antigen presenting cells.

the delivery of therapeutics to the brain [98,99,114,115]. Opening of the BBB upon intravenous administration of microbubbles and insonation at 1.63 MHz and 1 MPa was visualized in a rabbit model with magnetic resonance imaging (MRI) [116]. The mechanism behind microbubble-mediated BBB opening is dependent on microbubble size and acoustic intensity. Specifically, the BBB opening threshold at 1.5 MHz was 0.45 MPa for 1–2 μm microbubbles, and 0.3 MPa for 4–8 μm microbubbles. Since inertial cavitation in this system occurs above 0.45 MPa [116], the opening of the BBB with larger particles is not due to inertial cavitation.

Phase change perfluorocarbon nanodroplets have been shown to induce the opening of BBB upon exposure to focused ultrasound [117]. In mice, phase change perfluorobutane nanodroplets and fluorescent dextran were co-administered via tail vein injection. Insonation with focused ultrasound (1.5 MHz, 0.6 MPa, 5 min) caused a 7.4 fold increase in fluorescent dextran accumulation in the hippocampus compared to non-insonated animals, suggesting BBB opening.

Intravenously administered therapeutics that have demonstrated enhanced bioavailability to the brain upon co-administration of microbubbles and insonation range from small molecules [118] to antibodies [119] and nanoparticles [120]. Clinical studies have demonstrated the clinical feasibility of microbubble-mediated therapies. Low-intensity pulsed ultrasound in combination with microbubbles was found to increase chemotherapeutic accumulation in the brain in glioblastoma (GBM) in clinical trials. In a 2016 phase 1/2A clinical trial, intravenous administration of microbubbles was followed by insonation from an implantable device at an acoustic pressure $>$ 0.8 MPa, frequency 1 MHz [99]. BBB disruption was visualized in 28 of 41 patients by gadolinium contrast-enhanced MRI. A recent version of this implantable system, named SonoCloud-9, comprises nine ultrasound emitters, each operating at a frequency of 1 MHz (Fig. 2). In a 2023 dose-escalation phase I clinical trial, SonoCloud-9 achieved 3.7-fold and 5.9-fold increases in brain parenchymal drug concentrations of paclitaxel and carboplatin, respectively, when those albumin-bound drug were co-delivered with intravenous microbubbles [121]. Microbubble-mediated BBB opening was associated with mild to moderate neurological deficits, most commonly headache, moderately severe suppression of white blood cells, and hypertension. The chronic effects of BBB opening are unknown [122].

Microbubble-enhanced drug transport to the cerebral vasculature (rather than the brain itself) has been achieved without disruption of the BBB [123]. Using low-pressure focused ultrasound (FUS), they induced oscillation of cationic plasmid-conjugated microbubbles, facilitating endothelial cell membrane sonoporation. *In vivo*, systemic administration of DNA-conjugated microbubbles at 0.1 MPa pulse negative pressure (PNP), 1.1 MHz, resulted in 85–93 % endothelial-selective transfection after 24 h, with no observable inflammatory or immune responses. Magnetic resonance (MR) images showed no contrast agent extravasation into the brain, indicating no BBB disruption. The study suggests that acoustic sonoporation is effective at low FUS PNPs, enabling endothelial transfection without BBB disruption.

Microbubbles have also been found to enhance sciatic nerve block effectiveness upon co-administration (by local injection at the sciatic nerve) with the local anesthetic tetrodotoxin in a rat model [124]. The nerve block duration was enhanced three-fold with the co-administration of microbubbles and insonation (98 kPa). Histology showed no deleterious effects of ultrasound on tissue. These results suggest that the effects of microbubble cavitation upon insonation may

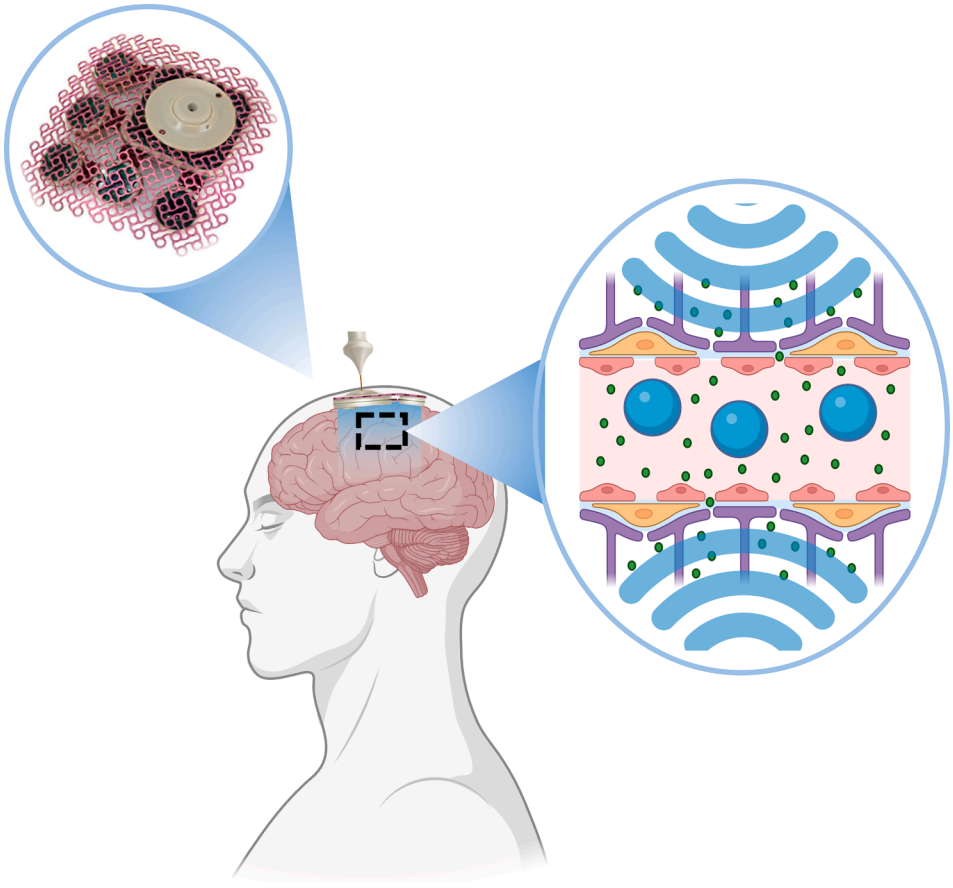

Fig. 2. Schematic of BBB opening with microbubbles upon insonation with an implantable ultrasound device (i.e., Sonocloud). Systemic co-administration of microbubbles with drugs induces BBB opening and enhances the accumulation of drugs in the target site. Illustrations were created with Biorender.com and adapted from [121], Elsevier 2023.

also assist drug penetration through peripheral nerve tissue barriers at low acoustic intensities.

Microbubbles may also be used to guide drug delivery systems to travel against blood flow upon insonation, demonstrated within the brain vasculature *in vivo* [125]. Lipid-coated microbubbles filled with sulfur hexafluoride gas aggregated upon insonation via secondary Bjerknes force. Ultrasound was transmitted through the mouse skull at 490 kHz and yielded a pressure range of 70 to 80 kPa. The aggregated complex (termed a microrobot in reference [125]) achieved upstream motion against blood flow, reaching velocities of 1.5 μm/s, and moving against blood flows of 10 mm/s. Safety concerns included vessel clogging in ~ 3 % of the analyzed vessels, primarily in small capillaries and venules, that recovered upon the cessation of ultrasound stimulation. Immunohistochemistry revealed no disruption of vascular endothelium or neuronal cell death. The potential risk from ultrasound-related hyperthermia remains to be assessed.

5.3. Ultrasound-triggered drug release from particulate drug delivery systems

Particulate drug delivery systems provide a strategy to overcome challenges in drug solubility, *in vivo* stability, and pharmacokinetics [126]. Ultrasound can further enhance the delivery efficiency of these systems. This section summarizes recent advances in the design of ultrasound-sensitive drug delivery systems for central and peripheral nervous system applications.

5.3.1. Microbubble-mediated particulate drug delivery systems

Microbubbles can be used as drug delivery agents. Chemotherapeutic doxorubicin was loaded into perfluoropropane-filled microbubbles [127]. Following intravenous administration of the doxorubicin-loaded microbubbles, focused ultrasound was transcranially applied in a rat model at 325 kPa, 400 kHz. Dye extravasation showed that the microbubbles induced BBB opening upon insonation. Doxorubicin accumulation in brain tissue was significantly enhanced when compared to areas not treated with ultrasound or animals administered with free doxorubicin.

Drug-loaded nanoparticles tethered onto microbubbles is another strategy for microbubble-mediated ultrasound-triggered drug delivery [128]. Gene-loaded adeno-associated viral vectors were covalently conjugated onto microbubbles for gene therapy [129]. Upon insonation with focused ultrasound *in vivo* (580 kHz, 0.4 MPa, 120 s), BBB opening was observed via MRI with a gadolinium-based contrast agent. The viral vectors were loaded with a gene associated with the neurorestoration of Parkinson's disease, SIRT3. After administration by tail-vein, followed by insonation of the striatum and substantia nigra, the SIRT3 gene was enhanced in the insonated regions.

Recently, the possibility of microbubble-mediated drug delivery to the brain without breaching the BBB has also been studied. A drug delivery system composed of microbubbles (~1.5 um) with drug-loaded liposomes (~120 nm) tethered to their surfaces, was insonated with a two-stage focused ultrasound sequence [130]. The first stage (0.075 MPa for 1 s/cycle) caused microbubble aggregation via secondary Bjerknes forces. The second stage (0.188 MPa for 90 ms/cycle) caused the local disruption of the tethered drug-loaded liposomes, inducing the release of the liposome-encapsulated drug. The authors hypothesized that ultrasound-induced aggregation of microbubbles in the brain vasculature via acoustic radiation. This aggregation could enhance ultrasound-triggered drug release due to enhanced shear effects induced by high velocity jets from collective microbubble gas release, mechanically destabilizing the liposomal lipid bilayers, inducing drug release. The authors found that both the aggregation and uncaging stages were required to induce effective drug release. The tethered liposomes were loaded with the psychoactive drug, muscimol. Insonation at 2.5 MHz ultrasound at 1000 cycles per treatment enabled the release of muscimol within the motor cortex in rats upon intravenous administration of the microbubble-liposome system. It achieved the inhibition of the vibrissae sensory-motor pathway without observable BBB opening or damage. The approach significantly reduced the required drug dose compared to systemic injection (1300x less), demonstrating the potential for ultrasound-induced localized drug delivery to effectively reduce off-target effects.

In contrast to the above examples, in which the microbubbles and the particles were administered systemically, microbubbles and drug-loaded particles have been co-delivered in a hydrogel, for ultrasound-triggered release. A mixture of microbubbles and dye-loaded liposomes contained in an in situ cross-linking hyaluronic acid hydrogel showed repeatable ultrasound-triggered dye release upon insonation [104]. The hydrogel system preserved proximity between the microbubble and dye-loaded liposomes, such that insonation would cause microbubble-mediated cavitation, which would enable dye release from liposomes. Ultrasound-triggered dye release was visible for up to 6 insonation events in a mouse model.

5.3.2. Phase change perfluorocarbon nanodroplets as drug delivery systems

Therapeutics can be loaded into phase change perfluorocarbon nanodroplets and released upon insonation. A lipophilic anesthetic pentobarbital was loaded into a commercial perfluoropropane microbubble contrast agent and condensed into liquid-filled nanodroplets [131] with a mean size of 210 nm. The pentobarbital-loaded nanodroplet was administered in rats via tail vein injection and the rat's motor cortices were insonated with focused ultrasound (0.58 MHz, 0.8 MPa, 5 s/min with 15 min total). A statistically significant motor deficit of 19.1 ± 13 % was observed by gait analysis, while the control groups (ultrasound only, and droplets without ultrasound) showed negligible differences.

5.3.3. Reactive oxygen species (ROS)-sensitive particulate drug delivery systems

Particulate carriers for sonochemistry-triggered drug release incorporate a ROS-sensitive element. Formulations containing unsaturated lipids can be chosen for this purpose, since singlet oxygen reacts with double bonds, causing lipid peroxidation, disrupting the stability of the nanocarrier and releasing the drug.

Repeatable ultrasound-triggered release of local anesthetics was achieved using ROS-sensitive liposomes (Fig. 3). Under insonation, the sonosensitizer protoporphyrin IX (PPIX) generated ROS (Fig. 3B), which induced peroxidation of the unsaturated lipid 1,2-dilinoleoyl-*sn*-glycero-3-phosphocholine (DLPC), which increased liposomal membrane permeability, allowing drug release [101]. Ultrasound-triggered release of encapsulated cargo was demonstrated *in vitro* and *in vivo* (Fig. 3C&D). The liposomes were loaded with the local anesthetic tetrodotoxin and injected at the rat sciatic nerve *in vivo*. Ultrasound-activated nerve block was demonstrated at 1 MHz, with the nerve block duration controllable via insonation intensity (1–3 W/cm^2) and duration (2–10 min). The ultrasound-activated nerve block could be repeated with subsequent insonation events after local anesthesia had worn off. The liposomes could be visualized by ultrasound imaging, demonstrating the potential to precisely monitor and locate the drug-delivering particles for on-demand, ultrasound-activated local anesthesia.

Lipid-based formulations without unsaturated lipids have also been reported to be ROS-sensitive. Pegylated liposomes containing a saturated phospholipid (i.e., hydrogenated soybean phosphatidylcholine) and cholesterol, loaded with the sonosensitizer hematoporphyrin monomethyl ether (HMME), demonstrated ultrasound sensitivity [68]. Insonation for a total of 120 s (10-s sonication followed by a 10-s pause at 1 MHz, 1.5 W·cm^{-2}) resulted in enhanced release of cargo (vincristine bitartrate). The same configuration containing the sonosensitizer Chlorin e6 resulted in ultrasound-triggered doxorubicin (DOX) release [67]. The mechanism of release was not elucidated.

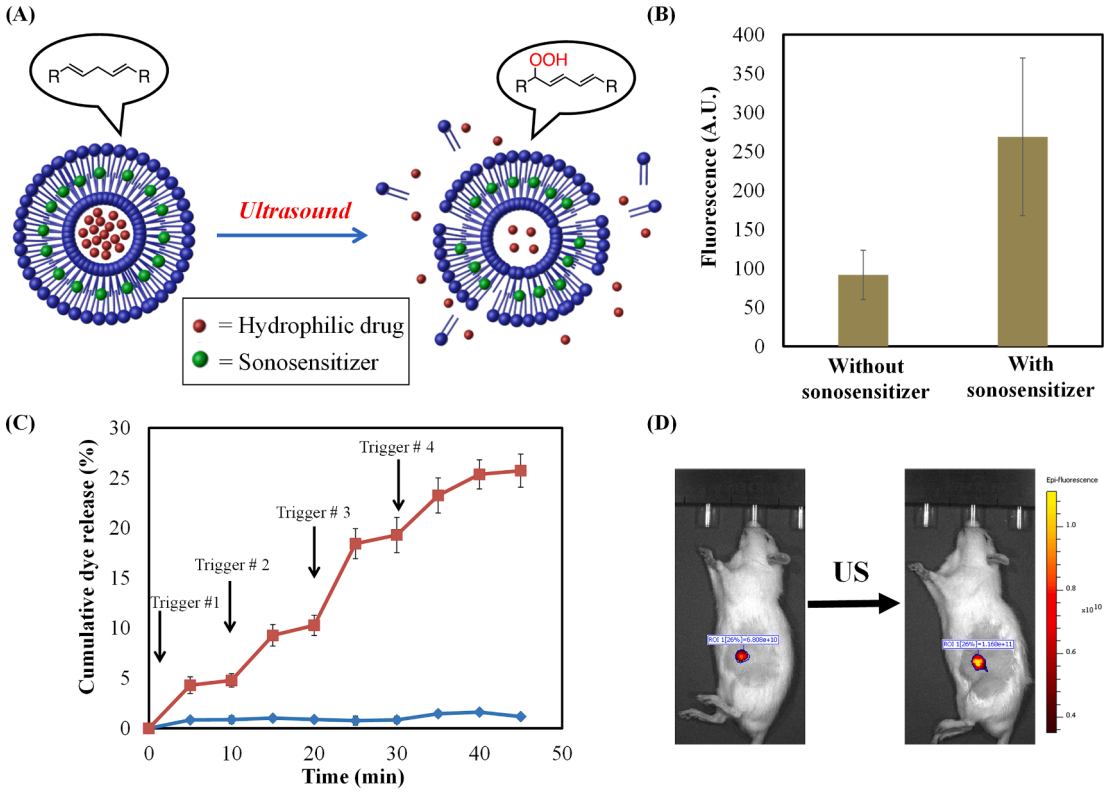

Fig. 3. Ultrasound-triggerable liposomes triggered by sonochemistry. (A) Schematic of ultrasound-sensitive liposomes. The liposomes are composed of lipids susceptible to ROS. Upon insonation, sonosensitizer-mediated ROS generation induces lipid peroxidation, thereby enhancing the permeability of the liposomes and releasing the encapsulated cargo. (B) Quantification of ROS generation using an ROS-specific fluorescent indicator, carboxy-H2DCFDA. A higher fluorescence indicates higher ROS generation. (C) Dye release kinetics, with and without insonation, from sonosensitizer-containing liposomes loaded with the fluorescent dye sulforhodamine B. red: with ultrasound; blue: without ultrasound. Each arrow represents insonation at 3 W/cm^2, 1 MHz, for 10 min. (D) Fluorescent image of a rat with subcutaneous injection of sonosensitizer-containing, dye-loaded, ultrasound-triggerable liposomes. The fluorescence intensity increased by 68.0 ± 17.1 % (mean, SD) after insonation. This enhancement demonstrates that cargo release from this system can be triggered by ultrasound *in vivo*. Left: before ultrasound (US), right: after ultrasound. Figures were adapted from [101], copyrighted by Nature Publishing Group; and [132], copyrighted by National Academy of Sciences, USA. (For interpretation of the references to color in this figure legend, the reader is referred to the web version of this article.)

5.3.4. *Polymeric drug delivery systems*

Polymer-based microcapsules, composed of a polymeric shell and an aqueous core, are sensitive to ultrasound due to the creation of defects on the polymeric shell upon insonation [133]. At high acoustic pressures (e.g., > 500 kPa) [134] the defects propagate, leading to the complete destruction of the polymeric shell. Lidocaine encapsulated within polylactic acid-glycolic acid microcapsules demonstrated ultrasound-triggered release [103]. The lidocaine-loaded microcapsules were percutaneously injected at the rat sciatic nerve in a model of sciatic nerve injury. Insonation resulted in drug release and pain relief.

6. Neuromodulation via insonation

Ultrasound itself has effects on the activity of neurons that are distinct from the above effects on drug delivery. Neuromodulation, the exposure of ultrasound to neurons, enables the control of neuron activity. For detailed information, we refer the reader to in-depth reviews on this topic [135–137].

Studies of neuromodulation suggest a number of potential mechanisms for the transient modulation of neural activity by ultrasound: (1) Neural membrane conformation change. The mechanical effects of ultrasound may alter membrane properties, such as thickness, curvature, and lipid molecule conformational states. This can result in a change in membrane capacitance (i.e., the speed at which the cell membrane potential reacts to the movement of ion channel currents), which can result in the excitation of neurons [138]. (2) Mechanosensitive channel activation. The activity of certain ion channels can be mechanically modulated by ultrasound, stimulating neural activity [139]. (3) Sonoporation. The formation of pores on cell membranes upon insonation can provide a transient channel for ion transport across the cell membrane, thereby changing neural activity. (4) Thermal effects. Temperature increases due to insonation can affect neural activity with two potential mechanisms [140,141]. First, the temperature-dependent transmembrane capacitance variation may induce capacitive currents, leading to depolarization and initiation of action potentials; second, increased temperature may activate temperature sensitive ion channels (e.g., TRPV1), thereby stimulating neuron activity. [142].

Clinical studies have suggested that neuromodulation may provide therapeutic effects. For the brain, a clinical study on chronic pain subjects found an improvement in mood after transcranial ultrasound energy (TUS) at 720 mW/cm^2, 8 MHz [143]. A number of clinical studies demonstrated improved cognitive, memory, and motor functions in patients with neurodegenerative dementia [144–146] upon insonation, with ultrasound conditions ranging between 2 and 4 MHz, and 0.5–3 W/cm^2. For the peripheral nervous system, insonation (2 MHz, 11.8 W/cm^2, < 2 s) of the fingertip of healthy subjects was found to activate somatosensory circuits in the brain, visualized via MRI [147]. No significant adverse effects were reported in these studies.

7. Systems and devices for ultrasound triggering

In recent years, the development of ultrasound-enhanced drug delivery technology has received increasing attention. However, its practical application has been hindered by the large size and weight of

conventional ultrasonic devices. Size/mass considerations are particularly important within the skull and spinal column, where there is limited space contained within non-expansile perimeters. The same constrains may be especially important in devices for particularly chronic diseases. Furthermore, tissues in the nervous system are mechanically soft, with a Young's modulus on the order of 1 kPa for the brain tissue [148]. Mechanically flexible device designs that match the mechanical properties of the nervous tissue is important for the safety of the device [149]. We will be focusing on ultrasonic systems for therapeutic applications; diagnostic systems have been reviewed elsewhere [150,151]. Such advances are important, even if the specific application to date is not in the nervous system.

7.1. Miniaturized ultrasound devices

Ultrasound is generated by ultrasonic transducers, including conventional piezoelectrics, capacitive micromachined ultrasound transducers (CMUTs), and piezoelectric micromachined ultrasound transducers (PMUTs). When an electrical voltage is applied, these ultrasound transducers generate high-frequency sound waves (>20 kHz) that propagate through tissues, inducing areas of expansion and contraction.

Transdermal drug delivery can be enhanced by portable ultrasound devices. Simultaneous combination of static pressure and ultrasound was enabled by a motor that provided static pressure (Fig. 4A, upper panel) and an ultrasonic transducer that provided an ultrasound wave of ~ 33 kHz at an estimated intensity of 100 mW/cm^2 (Fig. 4A, lower panel) [152]. The pressure from the motor could control the permeability of artificial skin to a dye (calcein), while ultrasound application further enhanced permeability. The combination of static pressure and ultrasound enhanced calcein permeability through artificial skin 2.6 fold, while ultrasound alone (without static pressure) enhanced the permeability 1.3 fold.

Miniaturized ultrasound devices have demonstrated potential in assisting drug penetration through the gastric mucosa, a barrier to orally administered drugs. A piezoelectric single crystal ultrasonic transducer (with a diameter of 2.2 mm) was made to generate sound waves of 6.9 MHz, 128 mW/cm^2 (Fig. 4B) [50]. The system was contained within an endoscope. *Ex vivo* studies showed a 5.6-fold increase in gastric mucosa permeability to bovine serum albumin upon insonation with this device. Such devices could be applied minimally invasively to enhance drug delivery across specific locations on the gastric mucosa.

Piezoelectric ceramic 3D printing is a manufacturing strategy that circumvents multi-step processing and design limitations of more conventional approaches (e.g., being limited to simple 2D geometries due to the mechanical brittleness of piezoelectric ceramic materials). The challenge of 3D printing, however, is that it often yields devices that have structural defects, leading to suboptimal performance when compared with traditional approaches. In a recent study, 3D printed piezoelectric transducers operating at ultrasonic frequencies of 9.75

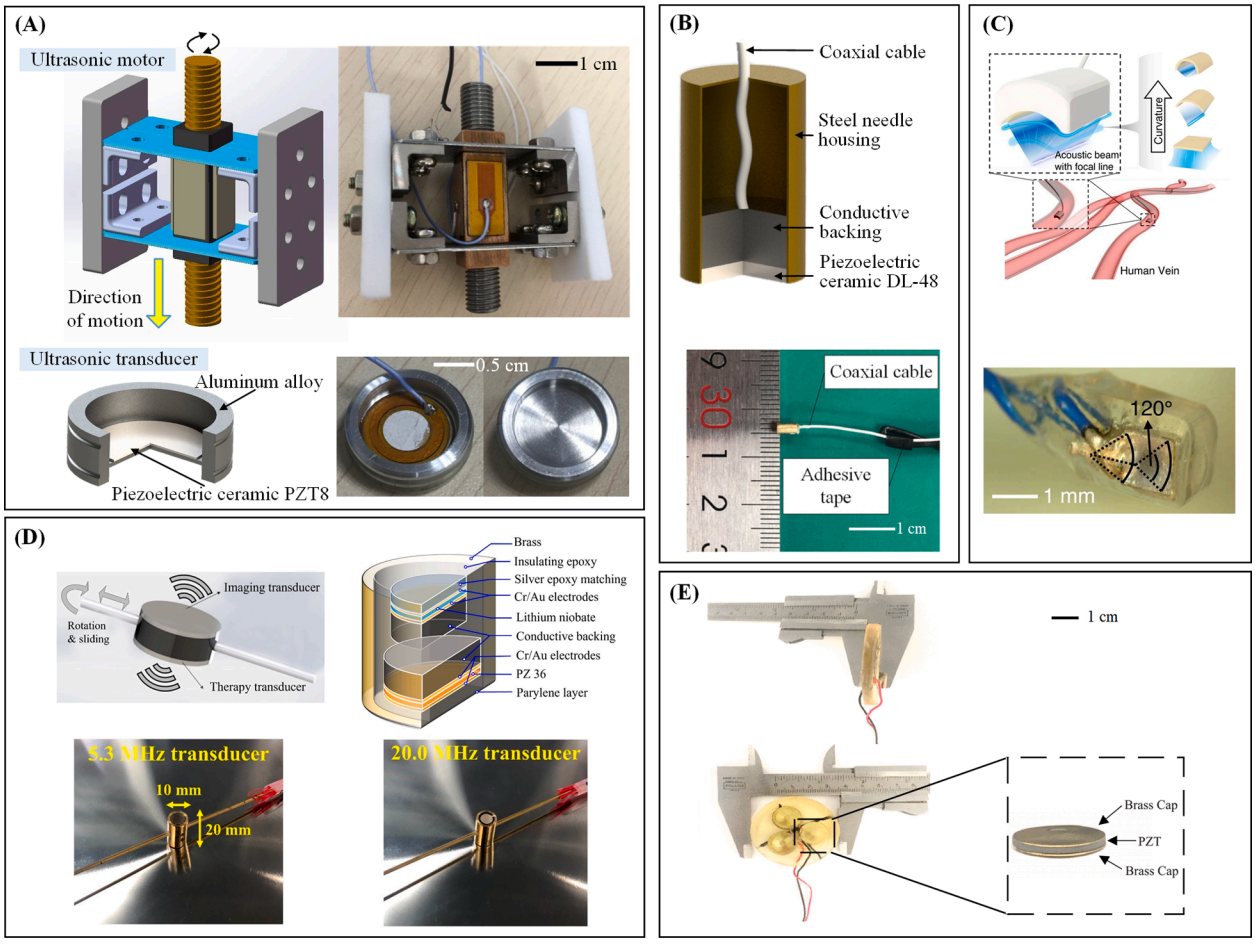

Fig. 4. Miniaturized ultrasonic transducers. (A) An ultrasonic transducer for non-invasive ultrasound transdermal drug delivery. (Adapted from [152], copyright 2018 IOP Publishing). (B) Piezoelectric single crystal ultrasonic transducer for endoscopic drug release to the gastric mucosa. (Adapted from [50], copyright 2021 IEEE). (C) Piezoelectric microtransducers for localized cavitation. (Adapted from [153], copyright 2023 The Author(s)). (D) An ultrasonic transducer that is capable to produce both therapeutic and diagnostic ultrasound in a single device, demonstrated for thermal ablation and high-resolution imaging. (Adapted from [154], copyright 2021 by the authors). (E) Low frequency ultrasound applicator for chronic wound treatment. (Adapted from [156], copyright 2019 IEEE).

MHz yielded high piezoelectric charge coefficient (electric charge generated per unit area with an applied mechanical force) comparable to traditional pristine ceramics (Fig. 4C) [153]. A drop of dye (methylene blue) was dropped in a microbubble solution to visualize diffusion.. Upon insonation, the diffusion coefficient was enhanced 6.4-fold by the presence of microbubbles, demonstrating the activation of cavitation and associated microbubble-mediated mechanical effects by the device. Bursting of microbubbles was also visualized in a 3D-printed transparent blood vessel phantom, demonstrating that the device generated sufficient acoustic energy to activate inertial cavitation.

Ultrasound imaging and treatment capabilities can be included within a single device [154]. High intensity focused ultrasound (HIFU) was achieved with a 5.3 MHz transducer, coupled with a 20 MHz transducer for high-resolution ultrasound imaging (Fig. 4D). The two inducers were placed back-to-back, enabling the device to achieve ultrasound imaging on one side and treatment on the other. The device induced coagulation necrosis (i.e., cell death due to lack of blood supply) *in vivo* with HIFU (>150 W/cm^2). The induced necrosis was visualized via the sonography enabled by the same device [155]. These results indicated the potential of such dual-mode (i.e., therapeutic and imaging) ultrasound device for subcutaneous thermal ablation and monitoring.

Miniaturized ultrasound devices have demonstrated therapeutic effects clinically. An ultrasound transducer designed for wound healing, 1 cm in thickness and 4 cm in diameter, generated an ultrasound intensity of 100 mW/cm^2 at 40 kHz (Fig. 4E) [156]. Upon placement on wound dressings in human subjects, insonation with this device shortened

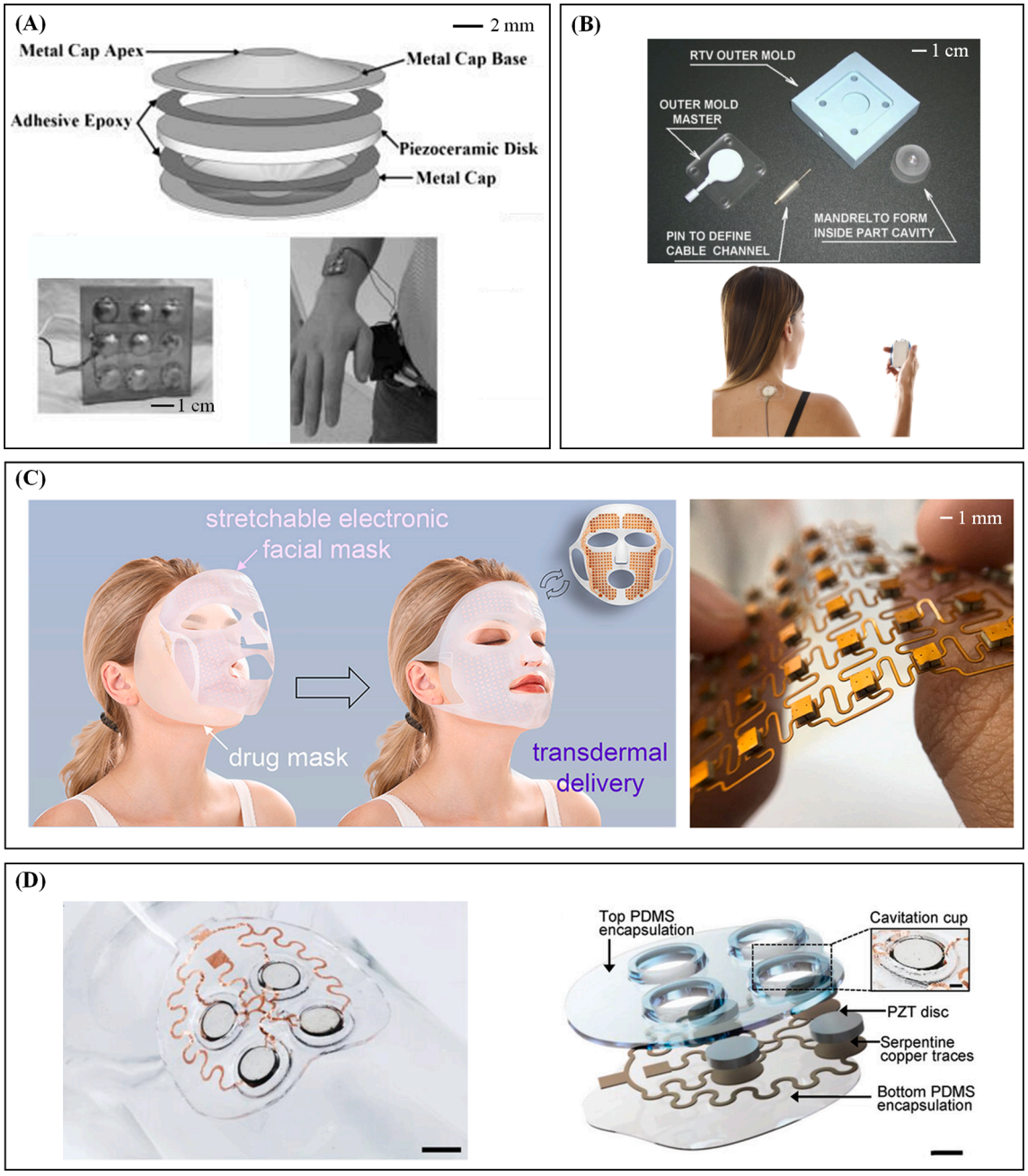

Fig. 5. Wearable ultrasound devices. (A) A flexional transducer for a fully portable ultrasound applicator. (Adapted from [158], copyright 2012 Published by Elsevier B.V.). (B) A wearable self-applied therapeutic ultrasound device for chronic myofascial pain. (Adapted from [159], copyright 2013 World Federation for Ultrasound in Medicine & Biology. Published by Elsevier Inc.). (C) Stretchable electronic facial mask for sonophoresis. (Adapted from [160], copyright 2022 American Chemical Society). (D) A conformable ultrasound patch for cavitation-enhanced transdermal cosmeceutical delivery. (Adapted from [162], copyright 2023 The Authors).

wound closure time from 12 weeks to 4.7 weeks.

7.2. Wearable ultrasound devices

Advances in electronics, actuators, and material engineering have led to the emergence of wireless on-demand drug delivery technologies [157]. Portable, miniaturized, and lightweight ultrasound devices have gained increasing interest due to their greater practicality in many contexts. Ultrasonic applicators could also be constructed with different numbers of individual transducer elements and customized geometries, to adjust their footprint or effective area. Minimizing the excitation voltage required to achieve the desired output could reduce the size of the power supply, allowing electronic devices and ultrasound applicators to be installed in wearable housings. A portable ultrasound applicator (Fig. 5A) could generate an ultrasound intensity of approximately 100 mW/cm^2 at an excitation voltage of 15 V, which indicates the possibility of powering via batteries [158].

Ultrasound therapy for musculoskeletal pain and healing is used daily in rehabilitation clinics. A wearable, battery-powered low-intensity therapeutic ultrasound device (Fig. 5B) was developed such that patients could self-apply ultrasound during daily activities. With a small, portable rechargeable battery (4.3 cm x 6.3 cm x 0.7 cm in size), it could operate for up to 6 h [159]. The system was evaluated in 30 patients on a prescription drug treatment regime for chronic trapezius myofascial pain. Those who used active ultrasound devices had an average pain reduction of 16 % after 1 h of treatment, compared with an average pain reduction of 8 % from those who used placebo (i.e., no ultrasound) devices.

An array of miniaturized piezoelectric transducers (1.0 × 1.0 × 1.3 mm^3 in size) were placed on the inner surface of a facial mask, designed for facial healthcare applications (Fig. 5C) [160]. The design could achieve a strain of 20 % and a Young's modulus of 600 kPa, demonstrating comparable mechanical properties to the human skin [161]. The matching of the mechanical properties between the device and the skin enabled the device to conform to the skin. Upon insonation *in vivo* in rats, the ultrasound device enhanced the penetration of hyaluronic acid delivery into skin. They further showed that the device could increase skin moisture content by 20 % in humans, likely due to the increased uptake of hyaluronic acid. Conformal ultrasound patches have also been used to enhance the transdermal transport of nicotinamide, a cosmeceutical compound (Fig. 5D) [162]. The system increased the flux of niacinamide across pig skin 26.2 fold after 10 min of ultrasound application.

7.3. Implantable ultrasound devices

A major challenge in the application of transcranial ultrasound is the high attenuation of the acoustic wave traveling through the thick human skull (5.3–7.5 mm [163]), hindering the delivery of ultrasound to the target brain region [164,165]. Implantable ultrasound devices may overcome this challenge by direct placement on the brain surface, bypassing the skull. Clinical studies with the implantable ultrasound system Sonocloud have demonstrated the potential of utilizing such systems in central nervous system diseases such as glioblastoma [121] (see *Section 5.2*).

As current devices require a second surgery to take out the device, biodegradability may be desirable. A biodegradable implantable ultrasound transducer has recently been developed with piezoelectric nanofibers of amino acid crystals [166]. Nanocrystals based on the amino acid glycine were electrospun in a polycaprolactone (PCL) biodegradable fiber, that created a piezoelectric film which emitted an acoustic pressure output of 334 kPa, 1 MHz, comparable to current commercialized transducers. *In vivo* Studies in animals with glioblastoma demonstrated that insonation of the brain with an implanted transducer (placed under the skull) after intravenous administration of microbubbles and the chemotherapeutic drug paclitaxel, increased survival time by up to two-fold compared to treatment without insonation [166].

8. Challenges and future perspectives of ultrasound-modulated drug delivery to the nervous system

Ultrasound is a promising technology to address challenges in drug delivery, including ineffective targeting and inadequate transport across physiological barriers. As in many fields of biomedical research, translation of ultrasound-triggered drug from small animals to humans will have to address the consequences of the enormous difference in size. For example, a mouse skull has a thickness of 0.1–0.65 mm [167], while the human skull is 5.3–7.5 mm thick [163], a difference that could have a marked impact on efficacy, given the high ultrasound attenuation coefficient of bone tissue (Table 1). Advances can be made, for example, by increasing the sensitivity of the drug delivery system to ultrasound, improving the efficiency of sonosensitizers, and developing more potent drugs or drug combinations (so that a greater therapeutic effect is released by a given insonation). The obstacle presented by anatomic features such as bone can be minimized or circumvented by implantable devices. The clinical importance of the benefit from such systems must be balanced against the potential clinical risks and additional costs.

Further studies into the long-term clinical safety of ultrasound-assisted drug delivery approaches will be beneficial to clinical translation. A system that combines both ultrasound imaging and ultrasound therapy capabilities may enable a real-time ultrasound-based feedback systems, in which ultrasound imaging can determine the precise location of the target tissue and/or drug delivery system for ultrasound triggered release. After treatment, the therapeutic effect can be monitored with ultrasound imaging. Such a system may mitigate safety concerns while optimizing therapeutic benefits by increasing drug concentrations in the targeted area.

Achieving long-lasting, portable ultrasound devices will be important, not only for wearables with flexible components. Repeated deformations caused by bending and stretching could result in mechanical degradation of the device, limiting its lifetime and leading to safety concerns; these potential problem should be addressed though advances in materials design and innovations in fabrication techniques [168]. These considerations will also be important for implantable devices, where matching of the mechanical properties of the device and the tissues could help prevent injury. Moreover, the minimization that would allow portability would also be important for implants, especially in relatively rigid enclosed spaces such as the inside of the skull.

Implantable ultrasound devices have gained traction due to their potential to provide accurate ultrasound dosages with high spatial resolution [169]. However, both implantable and wearable devices are associated with high power consumption. While the size and capacity of batteries have been greatly improved in the past few years, their lifespan is still limited. Furthermore, the volume of the battery usually accounts for 2/3 of the entire device volume. In the case of implantable devices, replacement of the depleted battery often necessitates surgery, which can increase hospitalization time and may entail clinical risk [170–172]. Strategies to extend battery lifetime by, for instance, developing application-specific integrated circuits that minimize the device's power consumption while harvesting the advantages of miniaturization may be a potential avenue to address such challenges. Another strategy may be to investigate alternative energy collection technologies. Implantable devices can be powered by external magnetic field, electromagnetic field, ultrasound, or infrared light [173,174].

Significant advances have been made in recent years in overcoming technical and pharmacological barriers associated with ultrasound-assisted drug delivery to the central and peripheral nervous system. For many of these, translation may require extensive validation prior to human testing, particularly since some will include a novel drug and/or drug delivery system and/or an ultrasound device. This combination of aspects may complicate the regulatory path to use in humans.

CRediT authorship contribution statement

Pancheng Zhu: Writing – original draft. **Ignasi Simon:** Writing – original draft. **Ida Kokalari:** Conceptualization. **Daniel S. Kohane:** Conceptualization, Supervision, Writing – review & editing. **Alina Y. Rwei:** Conceptualization, Supervision, Writing – original draft, Writing – review & editing.

Declaration of competing interest

The authors declare that they have no known competing financial interests or personal relationships that could have appeared to influence the work reported in this paper.

Data availability

No data was used for the research described in the article.

Acknowledgements

This work was funded by Delft University of Technology, Netherlands (A.Y.R., startup fund), the Hong Kong Polytechnic University, China (P.Z., Postdoc Matching Fund Scheme 2023/24, Grant Number 1-W31W), National Institutes of Health (NIH), United States, grant R35GM131728 (DSK)

References

[1] S. Sengupta, V.K. Balla, A review on the use of magnetic fields and ultrasound for non-invasive cancer treatment, J. Adv. Res. 14 (2018) 97–111, https://doi.org/10.1016/j.jare.2018.06.003.
[2] M.A. O'Reilly, K. Hynynen, Ultrasound enhanced drug delivery to the brain and central nervous system, Int. J. Hyperthermia 28 (2012) 386–396, https://doi.org/10.3109/02656736.2012.666709.
[3] N.J. Abbott, Dynamics of CNS barriers: evolution, differentiation, and modulation, Cell. Mol. Neurobiol. 25 (2005) 5–23, https://doi.org/10.1007/s10571-004-1374-y.
[4] E.E. Ubogu, Biology of the human blood-nerve barrier in health and disease, Exp. Neurol. 328 (2020) 113272, https://doi.org/10.1016/j.expneurol.2020.113272.
[5] J.B. Wang, T. Di Ianni, D.B. Vyas, Z. Huang, S. Park, N. Hosseini-Nassab, M. Aryal, R.D. Airan, Focused Ultrasound for Noninvasive, Focal Pharmacologic Neurointervention, Front. Neurosci. 14 (2020). https://www.frontiersin.org/articles/10.3389/fnins.2020.00675 (accessed November 17, 2023).
[6] Y. Meng, K. Hynynen, N. Lipsman, Applications of focused ultrasound in the brain: from thermoablation to drug delivery, Nat. Rev. Neurol. 17 (2021) 7–22, https://doi.org/10.1038/s41582-020-00418-z.
[7] C. Rabut, S. Yoo, R.C. Hurt, Z. Jin, H. Li, H. Guo, B. Ling, M.G. Shapiro, Ultrasound technologies for imaging and modulating neural activity, Neuron 108 (2020) 93–110, https://doi.org/10.1016/j.neuron.2020.09.003.
[8] Transcranial Focused Ultrasound for Noninvasive Neuromodulation of the Visual Cortex | IEEE Journals & Magazine | IEEE Xplore, (n.d.). https://ieeexplore.ieee.org/document/9127974 (accessed November 17, 2023).
[9] H.-M. Peng, P.-C. Zhu, Z.-J. Chen, Thermal analyses of in vitro low frequency sonophoresis, Ultrason. Sonochem. 35 (2017) 458–470, https://doi.org/10.1016/j.ultsonch.2016.10.027.
[10] Development of Implantable Medical Devices: From an Engineering Perspective, (n.d.). https://www.einj.org/journal/view.php?id=10.5213/inj.2013.17.3.98 (accessed November 17, 2023).
[11] S.J. Patey, J.P. Corcoran, Physics of ultrasound, Anaesth. Intensive Care Med. 22 (2021) 58–63, https://doi.org/10.1016/j.mpaic.2020.11.012.
[12] V.F. Humphrey, Ultrasound and matter—Physical interactions, Prog. Biophys. Mol. Biol. 93 (2007) 195–211, https://doi.org/10.1016/j.pbiomolbio.2006.07.024.
[13] J.P. Lefebvre, Chapter 1 - Physical Basis of Acoustics, in: P. Filippi, D. Habault, J.-P. Lefebvre, A. Bergassoli (Eds.), Acoustics, Academic Press, London, 1999: pp. 1–39. https://doi.org/10.1016/B978-012256190-0/50002-6.
[14] Diagnostic Radiology Physics: A Handbook for Teachers and Students, (n.d.).
[15] G. ter Haar, Ultrasonic imaging: Safety considerations, Interface, Focus 1 (2011) 686–697, https://doi.org/10.1098/rsfs.2011.0029.
[16] Statement on Biological Effects of Ultrasound in Vivo, Www.Aium.Org (n.d.). https://www.aium.org/resources/official-statements/view/statement-on-biological-effects-in-tissues-with-ultrasound-contrast-agents-2 (accessed December 8, 2023).
[17] Z. Izadifar, P. Babyn, D. Chapman, Mechanical and biological effects of ultrasound: a review of present knowledge, Ultrasound Med. Biol. 43 (2017) 1085–1104, https://doi.org/10.1016/j.ultrasmedbio.2017.01.023.
[18] Mechanical Bioeffects of Ultrasound | Annual Review of Biomedical Engineering, (n.d.). https://www.annualreviews.org/doi/abs/10.1146/annurev.bioeng.6.040803.140126 (accessed June 28, 2023).
[19] Potential Adverse Ultrasound-related Biological Effects | Anesthesiology | American Society of Anesthesiologists, (n.d.). https://pubs.asahq.org/anesthesiology/article/115/5/1109/12838/Potential-Adverse-Ultrasound-related-Biological (accessed July 11, 2023).
[20] M. Mischi, N.G. Rognin, M.A. Averkiou, 2.15 - Ultrasound Imaging Modalities, in: A. Brahme (Ed.), Compr. Biomed. Phys., Elsevier, Oxford, 2014: pp. 361–385. https://doi.org/10.1016/B978-0-444-53632-7.00217-3.
[21] C.M. Sehgal, J.F. Greenleaf, Ultrasonic absorption and dispersion in biological media: A postulated model, J. Acoust. Soc. Am. 72 (1982) 1711–1718, https://doi.org/10.1121/1.388664.
[22] P.N.T. Wells, Absorption and dispersion of ultrasound in biological tissue, Ultrasound Med. Biol. 1 (1975) 369–376, https://doi.org/10.1016/0301-5629(75)90124-6.
[23] A.D. Alarcon-Rojo, L.M. Carrillo-Lopez, R. Reyes-Villagrana, M. Huerta-Jiménez, I.A. Garcia-Galicia, Ultrasound and meat quality: A review, Ultrason. Sonochem. 55 (2019) 369–382, https://doi.org/10.1016/j.ultsonch.2018.09.016.
[24] A. Douplik, G. Saiko, I. Schelkanova, V.V. Tuchin, 3 - The response of tissue to laser light, in: H. Jelínková (Ed.), Lasers Med. Appl., Woodhead Publishing, 2013: pp. 47–109. https://doi.org/10.1533/9780857097545.1.47.
[25] C.A. Speed, Therapeutic ultrasound in soft tissue lesions, Rheumatol. Oxf. Engl. 40 (2001) 1331–1336, https://doi.org/10.1093/rheumatology/40.12.1331.
[26] Ultrasound Cavitation/Microbubble Detection and Medical Applications | SpringerLink, (n.d.). https://link.springer.com/article/10.1007/s40846-018-0391-0 (accessed June 28, 2023).
[27] C. Liang, J. Xie, S. Luo, C. Huang, Q. Zhang, H. Huang, P. Zhang, A highly potent ruthenium(II)-sonosensitizer and sonocatalyst for in vivo sonotherapy, Nat. Commun. 12 (2021) 5001, https://doi.org/10.1038/s41467-021-25303-1.
[28] C.-H. Fan, H.-L. Liu, C.-Y. Huang, Y.-J. Ma, T.-C. Yen, C.-K. Yeh, Detection of intracerebral hemorrhage and transient blood-supply shortage in focused-ultrasound-induced blood-brain barrier disruption by ultrasound imaging, Ultrasound Med. Biol. 38 (2012) 1372–1382, https://doi.org/10.1016/j.ultrasmedbio.2012.03.013.
[29] D. Miller, N. Smith, M. Bailey, G. Czarnota, K. Hynynen, I. Makin, Overview of therapeutic ultrasound applications and safety considerations, J. Ultrasound Med. Off. J. Am. Inst. Ultrasound Med. 31 (2012) 623–634.
[30] D. Needham, G. Anyarambhatla, G. Kong, M.W. Dewhirst, A new temperature-sensitive liposome for use with mild hyperthermia: characterization and testing in a human tumor xenograft model, Cancer Res. 60 (2000) 1197–1201.
[31] Multifunctional Thermosensitive Liposomes Based on Natural Phase-Change Material: Near-Infrared Light-Triggered Drug Release and Multimodal Imaging-Guided Cancer Combination Therapy | ACS Applied Materials & Interfaces, (n.d.). https://pubs.acs.org/doi/10.1021/acsami.8b22748 (accessed July 15, 2023).
[32] Thermal combination therapies for local drug delivery by magnetic resonance-guided high-intensity focused ultrasound | PNAS, (n.d.). https://www.pnas.org/doi/10.1073/pnas.1700790114 (accessed December 5, 2023).
[33] P.C. Lyon, M.D. Gray, C. Mannaris, L.K. Folkes, M. Stratford, L. Campo, D.Y. F. Chung, S. Scott, M. Anderson, R. Goldin, R. Carlisle, F. Wu, M.R. Middleton, F. V. Gleeson, C.C. Coussios, Safety and feasibility of ultrasound-triggered targeted drug delivery of doxorubicin from thermosensitive liposomes in liver tumours (TARDOX): a single-centre, open-label, phase 1 trial, Lancet Oncol. 19 (2018) 1027–1039, https://doi.org/10.1016/S1470-2045(18)30332-2.
[34] Theory and method of temperature control for drug release in hydrogel phantom of gastric mucosa in vitro | Journal of Applied Physics | AIP Publishing, (n.d.). https://pubs.aip.org/aip/jap/article/129/21/214506/158130/Theory-and-method-of-temperature-control-for-drug (accessed June 28, 2023).
[35] G.C. van Rhoon, M. Franckena, T.L.M. ten Hagen, A moderate thermal dose is sufficient for effective free and TSL based thermochemotherapy, Adv. Drug Deliv. Rev. 163–164 (2020) 145–156, https://doi.org/10.1016/j.addr.2020.03.006.
[36] R.E. Apfel, C.K. Holland, Gauging the likelihood of cavitation from short-pulse, low-duty cycle diagnostic ultrasound, Ultrasound Med. Biol. 17 (1991) 179–185, https://doi.org/10.1016/0301-5629(91)90125-g.
[37] M. Ashokkumar, The characterization of acoustic cavitation bubbles – An overview, Ultrason. Sonochem. 18 (2011) 864–872, https://doi.org/10.1016/j.ultsonch.2010.11.016.
[38] X. Guo, Q. Li, Z. Zhang, D. Zhang, J. Tu, Investigation on the inertial cavitation threshold and shell properties of commercialized ultrasound contrast agent microbubbles, J. Acoust. Soc. Am. 134 (2013) 1622–1631, https://doi.org/10.1121/1.4812887.
[39] H. Ueda, M. Mutoh, T. Seki, D. Kobayashi, Y. Morimoto, Acoustic cavitation as an enhancing mechanism of low-frequency sonophoresis for transdermal drug delivery, Biol. Pharm. Bull. 32 (2009) 916–920, https://doi.org/10.1248/bpb.32.916.
[40] Y. Li, D. Zhang, P. Zhang, Study on transdermal drug delivery with microneedle array, IOP Conf. Ser. Mater. Sci. Eng. 768 (2020) 052113, https://doi.org/10.1088/1757-899X/768/5/052113.
[41] C.K. Holland, R.E. Apfel, An improved theory for the prediction of microcavitation thresholds, IEEE Trans. Ultrason. Ferroelectr. Freq. Control 36 (1989) 204–208, https://doi.org/10.1109/58.19152.
[42] B.E. Polat, D. Hart, R. Langer, D. Blankschtein, Ultrasound-mediated transdermal drug delivery: Mechanisms, scope, and emerging trends, J. Control. Release 152 (2011) 330–348, https://doi.org/10.1016/j.jconrel.2011.01.006.
[43] S. Paliwal, G.K. Menon, S. Mitragotri, Low-frequency sonophoresis: ultrastructural basis for stratum corneum permeability assessed using quantum

dots, J. Invest. Dermatol. 126 (2006) 1095–1101, https://doi.org/10.1038/sj.jid.5700248.
[44] A. Tezel, S. Paliwal, Z. Shen, S. Mitragotri, Low-frequency ultrasound as a transcutaneous immunization adjuvant, Vaccine 23 (2005) 3800–3807, https://doi.org/10.1016/j.vaccine.2005.02.027.
[45] P. Dwivedi, S. Kiran, S. Han, M. Dwivedi, R. Khatik, R. Fan, F.A. Mangrio, K. Du, Z. Zhu, C. Yang, F. Huang, A. Ejaz, R. Han, T. Si, R.X. Xu, Magnetic targeting and ultrasound activation of liposome-microbubble conjugate for enhanced delivery of anticancer therapies, ACS Appl. Mater. Interfaces 12 (2020) 23737–23751, https://doi.org/10.1021/acsami.0c05308.
[46] Y.I. Yoon, Y.-S. Kwon, H.-S. Cho, S.-H. Heo, K.S. Park, S.G. Park, S.-H. Lee, S. I. Hwang, Y.I. Kim, H.J. Jae, G.-J. Ahn, Y.-S. Cho, H. Lee, H.J. Lee, T.-J. Yoon, Ultrasound-mediated gene and Drug delivery using a microbubble-liposome particle system, Theranostics 4 (2014) 1133–1144, https://doi.org/10.7150/thno.9945.
[47] F. Yan, L. Li, Z. Deng, Q. Jin, J. Chen, W. Yang, C.-K. Yeh, J. Wu, R. Shandas, X. Liu, H. Zheng, Paclitaxel-liposome–microbubble complexes as ultrasound-triggered therapeutic drug delivery carriers, J. Controlled Release 166 (2013) 246–255, https://doi.org/10.1016/j.jconrel.2012.12.025.
[48] S.V. Morse, A. Mishra, T.G. Chan, R.T.M. de Rosales, J.J. Choi, Liposome delivery to the brain with rapid short-pulses of focused ultrasound and microbubbles, J. Control. Release 341 (2022) 605–615, https://doi.org/10.1016/j.jconrel.2021.12.005.
[49] H.C. Starritt, F.A. Duck, V.F. Humphrey, An experimental investigation of streaming in pulsed diagnostic ultrasound beams, Ultrasound Med. Biol. 15 (1989) 363–373, https://doi.org/10.1016/0301-5629(89)90048-3.
[50] P. Zhu, H. Peng, L. Mao, J. Tian, Piezoelectric single crystal ultrasonic transducer for endoscopic drug release in gastric mucosa, IEEE Trans. Ultrason. Ferroelectr. Freq. Control 68 (2021) 952–960, https://doi.org/10.1109/TUFFC.2020.3026320.
[51] Modelling viscoacoustic wave propagation with the lattice Boltzmann method | Scientific Reports, (n.d.). https://www.nature.com/articles/s41598-017-10833-w (accessed June 28, 2023).
[52] Acoustic Wave Propagation in Complicated Geometries and Heterogeneous Media | SpringerLink, (n.d.). https://link.springer.com/article/10.1007/s10915-014-9817-1 (accessed June 28, 2023).
[53] H.J. Nieminen, T. Ylitalo, J.-P. Suuronen, K. Rahunen, A. Salmi, S. Saarakkala, R. Serimaa, E. Hæggström, Delivering agents locally into articular cartilage by intense MHz ultrasound, Ultrasound Med. Biol. 41 (2015) 2259–2265, https://doi.org/10.1016/j.ultrasmedbio.2015.03.025.
[54] S.R. Young, M. Dyson, The effect of therapeutic ultrasound on angiogenesis, Ultrasound Med. Biol. 16 (1990) 261–269, https://doi.org/10.1016/0301-5629(90)90005-W.
[55] Therapeutic ultrasound in soft tissue lesions | Rheumatology | Oxford Academic, (n.d.). https://academic.oup.com/rheumatology/article/40/12/1331/1787872?login=false (accessed June 28, 2023).
[56] A. Bystritsky, A.S. Korb, P.K. Douglas, M.S. Cohen, W.P. Melega, A. P. Mulgaonkar, A. DeSalles, B.-K. Min, S.-S. Yoo, A review of low-intensity focused ultrasound pulsation, Brain Stimulat. 4 (2011) 125–136, https://doi.org/10.1016/j.brs.2011.03.007.
[57] T.G. Leighton, A.J. Walton, M.J.W. Pickworth, Primary bjerknes forces, Eur. J. Phys. 11 (1990) 47, https://doi.org/10.1088/0143-0807/11/1/009.
[58] J.G.S. Moo, C.C. Mayorga-Martinez, H. Wang, W.Z. Teo, B.H. Tan, T.D. Luong, S. R. Gonzalez-Avila, C.-D. Ohl, M. Pumera, Bjerknes forces in motion: long-range translational motion and chiral directionality switching in bubble-propelled micromotors via an ultrasonic pathway, Adv. Funct. Mater. 28 (2018) 1702618, https://doi.org/10.1002/adfm.201702618.
[59] A.P. Sarvazyan, O.V. Rudenko, M. Fatemi, Acoustic radiation force: a review of four mechanisms for biomedical applications, IEEE Trans. Ultrason. Ferroelectr. Freq. Control 68 (2021) 3261–3269, https://doi.org/10.1109/TUFFC.2021.3112505.
[60] Y. Zhang, Y. Zhang, S. Li, The secondary bjerknes force between two gas bubbles under dual-frequency acoustic excitation, Ultrason. Sonochem. 29 (2016) 129–145, https://doi.org/10.1016/j.ultsonch.2015.08.022.
[61] A.P. Sarvazyan, O.V. Rudenko, W.L. Nyborg, Biomedical applications of radiation force of ultrasound: Historical roots and physical basis, Ultrasound Med. Biol. 36 (2010) 1379–1394, https://doi.org/10.1016/j.ultrasmedbio.2010.05.015.
[62] P.-K. Choi, Sonoluminescence and acoustic cavitation, Jpn. J. Appl. Phys. 56 (2017) 07JA01, https://doi.org/10.7567/JJAP.56.07JA01.
[63] M.P. Brenner, S. Hilgenfeldt, D. Lohse, Single-bubble sonoluminescence, Rev. Mod. Phys. 74 (2002) 425–484, https://doi.org/10.1103/RevModPhys.74.425.
[64] S. Li, G.S.P. Mok, Y. Dai, Lipid bilayer-based biological nanoplatforms for sonodynamic cancer therapy, Adv. Drug Deliv. Rev. 202 (2023) 115110, https://doi.org/10.1016/j.addr.2023.115110.
[65] S. Umemura, N. Yumita, R. Nishigaki, K. Umemura, Mechanism of cell damage by ultrasound in combination with hematoporphyrin, Jpn. J. Cancer Res. 81 (1990) 962–966, https://doi.org/10.1111/j.1349-7006.1990.tb02674.x.
[66] P. Riesz, D. Berdahl, C.L. Christman, Free radical generation by ultrasound in aqueous and nonaqueous solutions, Environ. Health Perspect. 64 (1985) 233–252, https://doi.org/10.1289/ehp.8564233.
[67] C. Zhou, X. Xie, H. Yang, S. Zhang, Y. Li, C. Kuang, S. Fu, L. Cui, M. Liang, C. Gao, Y. Yang, C. Gao, C. Yang, Novel class of ultrasound-triggerable drug delivery systems for the improved treatment of tumors, Mol. Pharm. 16 (2019) 2956–2965, https://doi.org/10.1021/acs.molpharmaceut.9b00194.
[68] W. Lin, X. Ma, C. Zhou, H. Yang, Y. Yang, X. Xie, C. Yang, C. Han, Development and characteristics of novel sonosensitive liposomes for vincristine bitartrate, Drug Deliv. 26 (2019) 724–731, https://doi.org/10.1080/10717544.2019.1639845.
[69] T.D. Lash, Origin of aromatic character in porphyrinoid systems, J. Porphyr. Phthalocyanines 15 (2011) 1093–1115, https://doi.org/10.1142/S1088424611004063.
[70] M. Yuan, S. Liang, Y. Zhou, X. Xiao, B. Liu, C. Yang, P. Ma, Z. Cheng, J. Lin, A robust oxygen-carrying hemoglobin-based natural sonosensitizer for sonodynamic cancer therapy, Nano Lett. 21 (2021) 6042–6050, https://doi.org/10.1021/acs.nanolett.1c01220.
[71] X. Geng, Y. Chen, Z. Chen, X. Wei, Y. Dai, Z. Yuan, Oxygen-carrying biomimetic nanoplatform for sonodynamic killing of bacteria and treatment of infection diseases, Ultrason. Sonochem. 84 (2022) 105972, https://doi.org/10.1016/j.ultsonch.2022.105972.
[72] X. Xing, S. Zhao, T. Xu, L. Huang, Y. Zhang, M. Lan, C. Lin, X. Zheng, P. Wang, Advances and perspectives in organic sonosensitizers for sonodynamic therapy, Coord. Chem. Rev. 445 (2021) 214087, https://doi.org/10.1016/j.ccr.2021.214087.
[73] X. Cao, M. Li, Q. Liu, J. Zhao, X. Lu, J. Wang, Inorganic sonosensitizers for sonodynamic therapy in cancer treatment, Small 19 (2023) 2303195, https://doi.org/10.1002/smll.202303195.
[74] N.J. Abbott, A.A.K. Patabendige, D.E.M. Dolman, S.R. Yusof, D.J. Begley, Structure and function of the blood–brain barrier, Neurobiol. Dis. 37 (2010) 13–25, https://doi.org/10.1016/j.nbd.2009.07.030.
[75] W.M. Pardridge, The blood-brain barrier: Bottleneck in brain drug development, NeuroRx 2 (2005) 3–14, https://doi.org/10.1602/neurorx.2.1.3.
[76] S. Peltonen, M. Alanne, J. Peltonen, Barriers of the peripheral nerve, Tissue Barriers 1 (2013) e24956.
[77] P. Lirk, M.W. Hollmann, G. Strichartz, The science of local anesthesia: basic research, clinical application, and future directions, Anesth. Analg. 126 (2018) 1381, https://doi.org/10.1213/ANE.0000000000002665.
[78] D. Hackel, S.M. Krug, R.-S. Sauer, S.A. Mousa, A. Böcker, D. Pflücke, E.-J. Wrede, K. Kistner, T. Hoffmann, B. Niedermirtl, C. Sommer, L. Bloch, O. Huber, I. E. Blasig, S. Amasheh, P.W. Reeh, M. Fromm, A. Brack, H.L. Rittner, Transient opening of the perineurial barrier for analgesic drug delivery, Proc. Natl. Acad. Sci. 109 (2012) E2018–E2027, https://doi.org/10.1073/pnas.1120800109.
[79] M. Kumar, R. Chawla, M. Goyal, Topical anesthesia, J. Anaesthesiol. Clin. Pharmacol. 31 (2015) 450, https://doi.org/10.4103/0970-9185.169049.
[80] M. Prausnitz, P. Elias, T. Franz, M. Schmuth, J. Tsai, G. Menon, W. Holleran, K. Feingold, Skin Barrier and Transdermal Drug Delivery, in: 2012. https://www.semanticscholar.org/paper/Skin-Barrier-and-Transdermal-Drug-Delivery-Prausnitz-Elias/effacec93496fdfd75c416a36c8414b15d8bcce1 (accessed November 26, 2023).
[81] W.M. Saltzman, Drug Permeation through Biological Barriers, in: W.M. Saltzman (Ed.), Drug Deliv. Eng. Princ. Drug Ther., Oxford University Press, 2001: p. 0. https://doi.org/10.1093/oso/9780195085891.003.0010.
[82] Z. Zhao, A. Ukidve, J. Kim, S. Mitragotri, Targeting strategies for tissue-specific drug delivery, Cell 181 (2020) 151–167, https://doi.org/10.1016/j.cell.2020.02.001.
[83] J. Tu, A.C.H. Yu, Ultrasound-Mediated Drug Delivery: Sonoporation Mechanisms, Biophysics, and Critical Factors, BME Front. 2022 (n.d.) 9807347. https://doi.org/10.34133/2022/9807347.
[84] S. Kotopoulis, A. Delalande, M. Popa, V. Mamaeva, G. Dimcevski, O.H. Gilja, M. Postema, B.T. Gjertsen, E. McCormack, Sonoporation-enhanced chemotherapy significantly reduces primary tumour burden in an orthotopic pancreatic cancer xenograft, Mol. Imaging Biol. 16 (2014) 53–62, https://doi.org/10.1007/s11307-013-0672-5.
[85] J. Wu, J. Pepe, M. Rincón, Sonoporation, anti-cancer drug and antibody delivery using ultrasound, Ultrasonics 44 (2006) e21–e25, https://doi.org/10.1016/j.ultras.2006.06.033.
[86] G. Shapiro, A.W. Wong, M. Bez, F. Yang, S. Tam, L. Even, D. Sheyn, S. Ben-David, W. Tawackoli, G. Pelled, K.W. Ferrara, D. Gazit, Multiparameter evaluation of in vivo gene delivery using ultrasound-guided, microbubble-enhanced sonoporation, J. Control. Release 223 (2016) 157–164, https://doi.org/10.1016/j.jconrel.2015.12.001.
[87] D. Park, H. Ryu, H.S. Kim, Y. Kim, K.-S. Choi, H. Park, J. Seo, Sonophoresis using ultrasound contrast agents for transdermal drug delivery: an in vivo experimental study, Ultrasound Med. Biol. 38 (2012) 642–650, https://doi.org/10.1016/j.ultrasmedbio.2011.12.015.
[88] D. Huang, M. Sun, Y. Bu, F. Luo, C. Lin, Z. Lin, Z. Weng, F. Yang, D. Wu, Microcapsule-embedded hydrogel patches for ultrasound responsive and enhanced transdermal delivery of diclofenac sodium, J. Mater. Chem. B 7 (2019) 2330–2337, https://doi.org/10.1039/C8TB02928H.
[89] S. Bhatnagar, J.J. Kwan, A.R. Shah, C.-C. Coussios, R.C. Carlisle, Exploitation of sub-micron cavitation nuclei to enhance ultrasound-mediated transdermal transport and penetration of vaccines, J. Control. Release 238 (2016) 22–30, https://doi.org/10.1016/j.jconrel.2016.07.016.
[90] Y.I. Svenskaya, E.A. Genina, B.V. Parakhonskiy, E.V. Lengert, E.E. Talnikova, G. S. Terentyuk, S.R. Utz, D.A. Gorin, V.V. Tuchin, G.B. Sukhorukov, A simple non-invasive approach toward efficient transdermal drug delivery based on biodegradable particulate system, ACS Appl. Mater. Interfaces 11 (2019) 17270–17282, https://doi.org/10.1021/acsami.9b04305.
[91] Y. Hu, M. Yang, H. Huang, Y. Shen, H. Liu, X. Chen, Controlled ultrasound erosion for transdermal delivery and hepatitis B immunization, Ultrasound Med. Biol. 45 (2019) 1208–1220, https://doi.org/10.1016/j.ultrasmedbio.2019.01.012.
[92] C.M. Schoellhammer, S. Srinivasan, R. Barman, S.H. Mo, B.E. Polat, R. Langer, D. Blankschtein, Applicability and safety of dual-frequency ultrasonic treatment

for the transdermal delivery of drugs, J. Control. Release 202 (2015) 93–100, https://doi.org/10.1016/j.jconrel.2015.02.002.
[93] B.M. Becker, S. Helfrich, E. Baker, K. Lovgren, P.A. Minugh, J.T. Machan, Ultrasound with topical anesthetic rapidly decreases pain of intravenous cannulation, Acad. Emerg. Med. 12 (2005) 289–295, https://doi.org/10.1197/j.aem.2004.11.019.
[94] N. Huebsch, C.J. Kearney, X. Zhao, J. Kim, C.A. Cezar, Z. Suo, D.J. Mooney, Ultrasound-triggered disruption and self-healing of reversibly cross-linked hydrogels for drug delivery and enhanced chemotherapy, Proc. Natl. Acad. Sci. 111 (2014) 9762–9767, https://doi.org/10.1073/pnas.1405469111.
[95] P. Wei, M. Sun, B. Yang, J. Xiao, J. Du, Ultrasound-responsive polymersomes capable of endosomal escape for efficient cancer therapy, J. Controlled Release 322 (2020) 81–94, https://doi.org/10.1016/j.jconrel.2020.03.013.
[96] A. Bar-Zion, A. Nourmahnad, D.R. Mittelstein, S. Shivaei, S. Yoo, M.T. Buss, R. C. Hurt, D. Malounda, M.H. Abedi, A. Lee-Gosselin, M.B. Swift, D. Maresca, M. G. Shapiro, Acoustically triggered mechanotherapy using genetically encoded gas vesicles, Nat. Nanotechnol. 16 (2021) 1403–1412, https://doi.org/10.1038/s41565-021-00971-8.
[97] A.V. Telichko, H. Wang, S. Bachawal, S.U. Kumar, J.C. Bose, R. Paulmurugan, J. J. Dahl, Therapeutic ultrasound parameter optimization for drug delivery applied to a murine model of hepatocellular carcinoma, Ultrasound Med. Biol. 47 (2021) 309–322, https://doi.org/10.1016/j.ultrasmedbio.2020.09.009.
[98] K. Beccaria, M. Canney, L. Goldwirt, C. Fernandez, J. Piquet, M.-C. Perier, C. Lafon, J.-Y. Chapelon, A. Carpentier, Ultrasound-induced opening of the blood-brain barrier to enhance temozolomide and irinotecan delivery: an experimental study in rabbits, J. Neurosurg. 124 (2016) 1602–1610, https://doi.org/10.3171/2015.4.JNS142893.
[99] A. Carpentier, M. Canney, A. Vignot, V. Reina, K. Beccaria, C. Horodyckid, C. Karachi, D. Leclercq, C. Lafon, J.-Y. Chapelon, L. Capelle, P. Cornu, M. Sanson, K. Hoang-Xuan, J.-Y. Delattre, A. Idbaih, Clinical trial of blood-brain barrier disruption by pulsed ultrasound, Sci. Transl. Med. 8 (2016) 343re2, https://doi.org/10.1126/scitranslmed.aaf6086.
[100] A.R. Rezai, P.-F. D'Haese, V. Finomore, J. Carpenter, M. Ranjan, K. Wilhelmsen, R.I. Mehta, P. Wang, U. Najib, C. Vieira Ligo Teixeira, T. Arsiwala, A. Tarabishy, P. Tirumalai, D.O. Claassen, S. Hodder, M.W. Haut, Ultrasound Blood–Brain Barrier Opening and Aducanumab in Alzheimer's Disease, N. Engl. J. Med. 390 (2024) 55–62. https://doi.org/10.1056/NEJMoa2308719.
[101] A.Y. Rwei, J.L. Paris, B. Wang, W. Wang, C.D. Axon, M. Vallet-Regí, R. Langer, D. S. Kohane, Ultrasound-triggered local anaesthesia, Nat. Biomed. Eng. 1 (2017) 644–653, https://doi.org/10.1038/s41551-017-0117-6.
[102] K. Cullion, L.C. Petishnok, T. Sun, C.M. Santamaria, G.L. Pemberton, N. J. McDannold, D.S. Kohane, Local anesthesia enhanced with increasing high-frequency ultrasound intensity, drug deliv, Transl. Res. 10 (2020) 1507–1516, https://doi.org/10.1007/s13346-020-00760-1.
[103] X. Xu, S. Chang, X. Zhang, T. Hou, H. Yao, S. Zhang, Y. Zhu, X. Cui, X. Wang, Fabrication of a controlled-release delivery system for relieving sciatica nerve pain using an ultrasound-responsive microcapsule, Front. Bioeng. Biotechnol. 10 (2022). https://www.frontiersin.org/articles/10.3389/fbioe.2022.1072205 (accessed November 18, 2023).
[104] H. Epstein-Barash, G. Orbey, B.E. Polat, R.H. Ewoldt, J. Feshitan, R. Langer, M. A. Borden, D.S. Kohane, A microcomposite hydrogel for repeated on-demand ultrasound-triggered drug delivery, Biomaterials 31 (2010) 5208–5217, https://doi.org/10.1016/j.biomaterials.2010.03.008.
[105] S. Wu, H. Zhang, S. Wang, J. Sun, Y. Hu, H. Liu, J. Liu, X. Chen, F. Zhou, L. Bai, X. Wang, J. Su, Ultrasound-triggered in situ gelation with ROS-controlled drug release for cartilage repair, Mater. Horiz. 10 (2023) 3507–3522, https://doi.org/10.1039/D3MH00042G.
[106] C.M. Schoellhammer, A. Schroeder, R. Maa, G.Y. Lauwers, A. Swiston, M. Zervas, R. Barman, A.M. DiCiccio, W.R. Brugge, D.G. Anderson, D. Blankschtein, R. Langer, G. Traverso, Ultrasound-mediated gastrointestinal drug delivery, Sci. Transl. Med. 7 (2015) 310ra168, https://doi.org/10.1126/scitranslmed.aaa5937.
[107] X. Li, S. Khorsandi, Y. Wang, J. Santelli, K. Huntoon, N. Nguyen, M. Yang, D. Lee, Y. Lu, R. Gao, B.Y.S. Kim, C. de Gracia Lux, R.F. Mattrey, W. Jiang, J. Lux, Cancer immunotherapy based on image-guided STING activation by nucleotide nanocomplex-decorated ultrasound microbubbles, Nat. Nanotechnol. 17 (2022) 891–899, https://doi.org/10.1038/s41565-022-01134-z.
[108] Thermo conductive carbon nanotube-framed membranes for skin heat signal-responsive transdermal drug delivery - Polymer Chemistry (RSC Publishing), (n. d.). https://pubs.rsc.org/en/content/articlelanding/2017/py/c7py00570a (accessed June 28, 2023).
[109] K. Tachibana, S. Tachibana, Use of ultrasound to enhance the local anesthetic effect of topically applied aqueous lidocaine, Anesthesiology 78 (1993) 1091–1096, https://doi.org/10.1097/00000542-199306000-00011.
[110] J.-M. Correas, L. Bridal, A. Lesavre, A. Méjean, M. Claudon, O. Hélénon, Ultrasound contrast agents: properties, principles of action, tolerance, and artifacts, Eur. Radiol. 11 (2001) 1316–1328, https://doi.org/10.1007/s003300100940.
[111] S. Schoen, M.S. Kilinc, H. Lee, Y. Guo, F.L. Degertekin, G.F. Woodworth, C. Arvanitis, Towards controlled drug delivery in brain tumors with microbubble-enhanced focused ultrasound, Adv. Drug Deliv. Rev. 180 (2022) 114043, https://doi.org/10.1016/j.addr.2021.114043.
[112] S. Ohta, E. Kikuchi, A. Ishijima, T. Azuma, I. Sakuma, T. Ito, Investigating the optimum size of nanoparticles for their delivery into the brain assisted by focused ultrasound-induced blood–brain barrier opening, Sci. Rep. 10 (2020) 18220, https://doi.org/10.1038/s41598-020-75253-9.
[113] W. Zhang, Y. Shi, S.A. Shukor, A. Vijayakumaran, S. Vlatakis, M. Wright, M. Thanou, Phase-shift nanodroplets as an emerging sonoresponsive nanomaterial for imaging and drug delivery applications, Nanoscale 14 (2022) 2943–2965, https://doi.org/10.1039/D1NR07882H.
[114] M. Aryal, N. Vykhodtseva, Y.-Z. Zhang, J. Park, N. McDannold, Multiple treatments with liposomal doxorubicin and ultrasound-induced disruption of blood–tumor and blood–brain barriers improve outcomes in a rat glioma model, J. Control. Release 169 (2013) 103–111, https://doi.org/10.1016/j.jconrel.2013.04.007.
[115] K. Beccaria, M. Canney, L. Goldwirt, C. Fernandez, C. Adam, J. Piquet, G. Autret, O. Clément, C. Lafon, J.-Y. Chapelon, A. Carpentier, Opening of the blood-brain barrier with an unfocused ultrasound device in rabbits: laboratory investigation, J. Neurosurg. 119 (2013) 887–898, https://doi.org/10.3171/2013.5.JNS122374.
[116] K. Hynynen, N. McDannold, N. Vykhodtseva, F.A. Jolesz, Noninvasive MR imaging–guided focal opening of the blood-brain barrier in rabbits, Radiology 220 (2001) 640–646, https://doi.org/10.1148/radiol.2202001804.
[117] C.C. Chen, P.S. Sheeran, S.-Y. Wu, O.O. Olumolade, P.A. Dayton, E.E. Konofagou, Targeted drug delivery with focused ultrasound-induced blood-brain barrier opening using acoustically-activated nanodroplets, J. Control. Release 172 (2013) 795–804, https://doi.org/10.1016/j.jconrel.2013.09.025.
[118] Z. Kovacs, B. Werner, A. Rassi, J.O. Sass, E. Martin-Fiori, M. Bernasconi, Prolonged survival upon ultrasound-enhanced doxorubicin delivery in two syngenic glioblastoma mouse models, J. Control. Release 187 (2014) 74–82, https://doi.org/10.1016/j.jconrel.2014.05.033.
[119] T. Kobus, I.K. Zervantonakis, Y. Zhang, N.J. McDannold, Growth inhibition in a brain metastasis model by antibody delivery using focused ultrasound-mediated blood-brain barrier disruption, J. Controlled Release 238 (2016) 281–288, https://doi.org/10.1016/j.jconrel.2016.08.001.
[120] T. Sun, Y. Zhang, C. Power, P.M. Alexander, J.T. Sutton, M. Aryal, N. Vykhodtseva, E.L. Miller, N.J. McDannold, Closed-loop control of targeted ultrasound drug delivery across the blood–brain/tumor barriers in a rat glioma model, Proc. Natl. Acad. Sci. 114 (2017) E10281–E10290, https://doi.org/10.1073/pnas.1713328114.
[121] A.M. Sonabend, A. Gould, C. Amidei, R. Ward, K.A. Schmidt, D.Y. Zhang, C. Gomez, J.F. Bebawy, B.P. Liu, G. Bouchoux, C. Desseaux, I.B. Helenowski, R. V. Lukas, K. Dixit, P. Kumthekar, V.A. Arrieta, M.S. Lesniak, A. Carpentier, H. Zhang, M. Muzzio, M. Canney, R. Stupp, Repeated blood–brain barrier opening with an implantable ultrasound device for delivery of albumin-bound paclitaxel in patients with recurrent glioblastoma: a phase 1 trial, Lancet Oncol. 24 (2023) 509–522, https://doi.org/10.1016/S1470-2045(23)00112-2.
[122] Z.I. Kovacs, S. Kim, N. Jikaria, F. Qureshi, B. Milo, B.K. Lewis, M. Bresler, S. R. Burks, J.A. Frank, Disrupting the blood–brain barrier by focused ultrasound induces sterile inflammation, Proc. Natl. Acad. Sci. 114 (2017), https://doi.org/10.1073/pnas.1614777114.
[123] C.M. Gorick, A.S. Mathew, W.J. Garrison, E.A. Thim, D.G. Fisher, C.A. Copeland, J. Song, A.L. Klibanov, G.W. Miller, R.J. Price, Sonoselective transfection of cerebral vasculature without blood–brain barrier disruption, Proc. Natl. Acad. Sci. 117 (2020) 5644–5654, https://doi.org/10.1073/pnas.1914595117.
[124] K. Cullion, C.M. Santamaria, C. Zhan, D. Zurakowski, T. Sun, G.L. Pemberton, N. J. McDannold, D.S. Kohane, High-frequency, low-intensity ultrasound and microbubbles enhance nerve blockade, J. Controlled Release 276 (2018) 150–156, https://doi.org/10.1016/j.jconrel.2018.02.027.
[125] A. Del Campo Fonseca, C. Glück, J. Droux, Y. Ferry, C. Frei, S. Wegener, B. Weber, M. El Amki, D. Ahmed, Ultrasound trapping and navigation of microrobots in the mouse brain vasculature, Nat. Commun. 14 (2023) 5889, https://doi.org/10.1038/s41467-023-41557-3.
[126] D.S. Kohane, Microparticles and nanoparticles for drug delivery, Biotechnol. Bioeng. 96 (2007) 203–209, https://doi.org/10.1002/bit.21301.
[127] C.-H. Fan, C.-Y. Ting, H.-J. Lin, C.-H. Wang, H.-L. Liu, T.-C. Yen, C.-K. Yeh, SPIO-conjugated, doxorubicin-loaded microbubbles for concurrent MRI and focused-ultrasound enhanced brain-tumor drug delivery, Biomaterials 34 (2013) 3706–3715, https://doi.org/10.1016/j.biomaterials.2013.01.099.
[128] S.R. Sirsi, M.A. Borden, State-of-the-art materials for ultrasound-triggered drug delivery, Adv. Drug Deliv. Rev. 72 (2014) 3–14, https://doi.org/10.1016/j.addr.2013.12.010.
[129] D. Trinh, J. Nash, D. Goertz, K. Hynynen, S. Bulner, U. Iqbal, J. Keenan, Microbubble drug conjugate and focused ultrasound blood brain barrier delivery of AAV-2 SIRT-3, Drug Deliv. 29 (2022) 1176–1183, https://doi.org/10.1080/10717544.2022.2035855.
[130] M.S. Ozdas, A.S. Shah, P.M. Johnson, N. Patel, M. Marks, T.B. Yasar, U. Stalder, L. Bigler, W. von der Behrens, S.R. Sirsi, M.F. Yanik, Non-invasive molecularly-specific millimeter-resolution manipulation of brain circuits by ultrasound-mediated aggregation and uncaging of drug carriers, Nat. Commun. 11 (2020) 4929, https://doi.org/10.1038/s41467-020-18059-7.
[131] H. Lea-Banks, M.A. O'Reilly, C. Hamani, K. Hynynen, Localized anesthesia of a specific brain region using ultrasound-responsive barbiturate nanodroplets, Theranostics 10 (2020) 2849–2858, https://doi.org/10.7150/thno.41566.
[132] A.Y. Rwei, J.-J. Lee, C. Zhan, Q. Liu, M.T. Ok, S.A. Shankarappa, R. Langer, D. S. Kohane, Repeatable and adjustable on-demand sciatic nerve block with phototriggerable liposomes, Proc. Natl. Acad. Sci. 112 (2015) 15719–15724, https://doi.org/10.1073/pnas.1518791112.
[133] K.W. Jang, D. Seol, L. Ding, D.N. Heo, S.J. Lee, J.A. Martin, I.K. Kwon, Ultrasound-triggered PLGA microparticle destruction and degradation for controlled delivery of local cytotoxicity and drug release, Int. J. Biol. Macromol. 106 (2018) 1211–1217, https://doi.org/10.1016/j.ijbiomac.2017.08.125.

[134] S.H. Bloch, M. Wan, P.A. Dayton, K.W. Ferrara, Optical observation of lipid- and polymer-shelled ultrasound microbubble contrast agents, Appl. Phys. Lett. 84 (2004) 631–633, https://doi.org/10.1063/1.1643544.
[135] H.A.S. Kamimura, A. Conti, N. Toschi, E.E. Konofagou, Ultrasound Neuromodulation: Mechanisms and the Potential of Multimodal Stimulation for Neuronal Function Assessment, Front. Phys. 8 (2020). https://www.frontiersin.org/articles/10.3389/fphy.2020.00150 (accessed December 5, 2023).
[136] T. Liu, M.H. Choi, J. Zhu, T. Zhu, J. Yang, N. Li, Z. Chen, Q. Xian, X. Hou, D. He, J. Guo, C. Fei, L. Sun, Z. Qiu, Sonogenetics: Recent advances and future directions, Brain Stimulat. 15 (2022) 1308–1317, https://doi.org/10.1016/j.brs.2022.09.002.
[137] F. Yang, S.-J. Kim, X. Wu, H. Cui, S.K. Hahn, G. Hong, Principles and applications of sono-optogenetics, Adv. Drug Deliv. Rev. 194 (2023) 114711, https://doi.org/10.1016/j.addr.2023.114711.
[138] M.G. Shapiro, K. Homma, S. Villarreal, C.-P. Richter, F. Bezanilla, Infrared light excites cells by changing their electrical capacitance, Nat. Commun. 3 (2012) 736, https://doi.org/10.1038/ncomms1742.
[139] W.J. Tyler, The mechanobiology of brain function, Nat. Rev. Neurosci. 13 (2012) 867–878, https://doi.org/10.1038/nrn3383.
[140] S.M. Thompson, L.M. Masukawa, D.A. Prince, Temperature dependence of intrinsic membrane properties and synaptic potentials in hippocampal CA1 neurons in vitro, J. Neurosci. 5 (1985) 817–824, https://doi.org/10.1523/JNEUROSCI.05-03-00817.1985.
[141] S. Luan, I. Williams, K. Nikolic, T.G. Constandinou, Neuromodulation: present and emerging methods, Front. Neuroengineering 7 (2014). https://www.frontiersin.org/articles/10.3389/fneng.2014.00027 (accessed February 19, 2024).
[142] O. Karatum, M. Han, E.T. Erdogan, S. Karamursel, S. Nizamoglu, Physical mechanisms of emerging neuromodulation modalities, J. Neural Eng. 20 (2023) 031001, https://doi.org/10.1088/1741-2552/acd870.
[143] S. Hameroff, M. Trakas, C. Duffield, E. Annabi, M.B. Gerace, P. Boyle, A. Lucas, Q. Amos, A. Buadu, J.J. Badal, Transcranial ultrasound (TUS) effects on mental states: a pilot study, Brain Stimulat. 6 (2013) 409–415, https://doi.org/10.1016/j.brs.2012.05.002.
[144] N.E. Nicodemus, S. Becerra, T.P. Kuhn, H.R. Packham, J. Duncan, K. Mahdavi, J. Iovine, S. Kesari, S. Pereles, M. Whitney, M. Mamoun, D. Franc, A. Bystritsky, S. Jordan, Focused transcranial ultrasound for treatment of neurodegenerative dementia, Alzheimers Dement. Transl. Res. Clin. Interv. 5 (2019) 374–381, https://doi.org/10.1016/j.trci.2019.06.007.
[145] R. Beisteiner, E. Matt, C. Fan, H. Baldysiak, M. Schönfeld, T. Philippi Novak, A. Amini, T. Aslan, R. Reinecke, J. Lehrner, A. Weber, U. Reime, C. Goldenstedt, E. Marlinghaus, M. Hallett, H. Lohse-Busch, Transcranial pulse stimulation with ultrasound in alzheimer's disease—A new navigated focal brain therapy, Adv. Sci. 7 (2020) 1902583, https://doi.org/10.1002/advs.201902583.
[146] H. Jeong, J.J. Im, J.-S. Park, S.-H. Na, W. Lee, S.-S. Yoo, I.-U. Song, Y.-A. Chung, Ultrasonography, Ultrasonography 40 (2021) 512–519, https://doi.org/10.14366/usg.20138.
[147] W. Legon, A. Rowlands, A. Opitz, T.F. Sato, W.J. Tyler, Pulsed ultrasound differentially stimulates somatosensory circuits in humans as indicated by EEG and fMRI, PLoS One 7 (2012) e51177.
[148] S. Budday, R. Nay, R. de Rooij, P. Steinmann, T. Wyrobek, T.C. Ovaert, E. Kuhl, Mechanical properties of gray and white matter brain tissue by indentation, J. Mech. Behav. Biomed. Mater. 46 (2015) 318–330, https://doi.org/10.1016/j.jmbbm.2015.02.024.
[149] E. Song, J. Li, S.M. Won, W. Bai, J.A. Rogers, Materials for flexible bioelectronic systems as chronic neural interfaces, Nat. Mater. 19 (2020) 590–603, https://doi.org/10.1038/s41563-020-0679-7.
[150] C. Wang, X. Chen, L. Wang, M. Makihata, H.-C. Liu, T. Zhou, X. Zhao, Bioadhesive ultrasound for long-term continuous imaging of diverse organs, Science 377 (2022) 517–523, https://doi.org/10.1126/science.abo2542.
[151] H. Hu, H. Huang, M. Li, X. Gao, L. Yin, R. Qi, R.S. Wu, X. Chen, Y. Ma, K. Shi, C. Li, T.M. Maus, B. Huang, C. Lu, M. Lin, S. Zhou, Z. Lou, Y. Gu, Y. Chen, Y. Lei, X. Wang, R. Wang, W. Yue, X. Yang, Y. Bian, J. Mu, G. Park, S. Xiang, S. Cai, P. W. Corey, J. Wang, S. Xu, A wearable cardiac ultrasound imager, Nature 613 (2023) 667–675, https://doi.org/10.1038/s41586-022-05498-z.
[152] A New Low-frequency Sonophoresis System Combined with Ultrasonic Motor and Transducer - IOPscience, (n.d.). https://iopscience.iop.org/article/10.1088/1361-665X/aaad9c (accessed June 28, 2023).
[153] 3D Printing and processing of miniaturized transducers with near-pristine piezoelectric ceramics for localized cavitation | Nature Communications, (n.d.). https://www.nature.com/articles/s41467-023-37335-w#Abs1 (accessed June 28, 2023).
[154] L. Hg, K. H, K. K, P. J, K. Y, Y. J, H. D, B. J, P. Sm, K. Hh, Thermal Ablation and High-Resolution Imaging Using a Back-to-Back (BTB) Dual-Mode Ultrasonic Transducer: In Vivo Results, Sensors 21 (2021). https://doi.org/10.3390/s21051580.
[155] T.L. Szabo, Chapter 8 - Wave Scattering and Imaging, in: T.L. Szabo (Ed.), Diagn. Ultrasound Imaging Second Ed., Academic Press, Boston, 2014: pp. 257–294. https://doi.org/10.1016/B978-0-12-396487-8.00008-2.
[156] O. Ngo, E. Niemann, V. Gunasekaran, P. Sankar, M. Putterman, A. Lafontant, S. Nadkarni, R.A. Dimaria-Ghalili, M. Neidrauer, L. Zubkov, M. Weingarten, D. J. Margolis, P.A. Lewin, Development of low frequency (20–100 kHz) clinically viable ultrasound applicator for chronic wound treatment, IEEE Trans. Ultrason. Ferroelectr. Freq. Control 66 (2019) 572–580, https://doi.org/10.1109/TUFFC.2018.2836311.
[157] Drugs go wireless | Nature Biotechnology, (n.d.). https://www.nature.com/articles/nbt.3446 (accessed June 28, 2023).
[158] C.R. Bawiec, Y. Sunny, A.T. Nguyen, J.A. Samuels, M.S. Weingarten, L.A. Zubkov, P.A. Lewin, Finite element static displacement optimization of 20–100kHz flexural transducers for fully portable ultrasound applicator, Ultrasonics 53 (2013) 511–517, https://doi.org/10.1016/j.ultras.2012.09.005.
[159] G.K. Lewis, M.D. Langer, C.R. Henderson, R. Ortiz, Design and evaluation of a wearable self-applied therapeutic ultrasound device for chronic myofascial pain, Ultrasound Med. Biol. 39 (2013) 1429–1439, https://doi.org/10.1016/j.ultrasmedbio.2013.03.007.
[160] Stretchable Electronic Facial Masks for Sonophoresis | ACS Nano, (n.d.). https://pubs.acs.org/doi/10.1021/acsnano.1c11181?ref=pdf (accessed June 28, 2023).
[161] M. Pawlaczyk, M. Lelonkiewicz, M. Wieczorowski, Age-dependent biomechanical properties of the skin, Adv. Dermatol. Allergol. Dermatol. Alergol. 30 (2013) 302–306, https://doi.org/10.5114/pdia.2013.38359.
[162] C.-C. Yu, A. Shah, N. Amiri, C. Marcus, M.O.G. Nayeem, A.K. Bhayadia, A. Karami, C. Dagdeviren, A conformable ultrasound patch for cavitation-enhanced transdermal cosmeceutical delivery, Adv. Mater. Deerfield Beach Fla 35 (2023) e2300066, https://doi.org/10.1002/adma.202300066.
[163] A. Moreira-Gonzalez, F.E. Papay, J.E. Zins, Calvarial thickness and its relation to cranial bone harvest, Plast. Reconstr. Surg. 117 (2006) 1964, https://doi.org/10.1097/01.prs.0000209933.78532.a7.
[164] F.J. Fry, J.E. Barger, Acoustical properties of the human skull, J. Acoust. Soc. Am. 63 (1978) 1576–1590, https://doi.org/10.1121/1.381852.
[165] G. Pinton, J.-F. Aubry, E. Bossy, M. Muller, M. Pernot, M. Tanter, Attenuation, scattering, and absorption of ultrasound in the skull bone, Med. Phys. 39 (2012) 299–307, https://doi.org/10.1118/1.3668316.
[166] M.T. Chorsi, T.T. Le, F. Lin, T. Vinikoor, R. Das, J.F. Stevens, C. Mundrane, J. Park, K.T.M. Tran, Y. Liu, J. Pfund, R. Thompson, W. He, M. Jain, M. D. Morales-Acosta, O.R. Bilal, K. Kazerounian, H. Ilies, T.D. Nguyen, Highly piezoelectric, biodegradable, and flexible amino acid nanofibers for medical applications, Sci. Adv. 9 (2023) eadg6075, https://doi.org/10.1126/sciadv.adg6075.
[167] L. Ghanbari, M.L. Rynes, J. Hu, D.S. Schulman, G.W. Johnson, M. Laroque, G. M. Shull, S.B. Kodandaramaiah, Craniobot: A computer numerical controlled robot for cranial microsurgeries, Sci. Rep. 9 (2019) 1023, https://doi.org/10.1038/s41598-018-37073-w.
[168] H. Huang, R.S. Wu, M. Lin, S. Xu, Emerging wearable ultrasound technology, IEEE Trans. Ultrason. Ferroelectr. Freq. Control (2023) 1, https://doi.org/10.1109/TUFFC.2023.3327143.
[169] Implantable batteryless device for on-demand and pulsatile insulin administration | Nature Communications, (n.d.). https://www.nature.com/articles/ncomms15032 (accessed June 28, 2023).
[170] R. Sobot, Implantable systems – Retrospective tutorial review, Microelectron. J. 88 (2019) 190–198, https://doi.org/10.1016/j.mejo.2017.10.001.
[171] C. Camara, P. Peris-Lopez, J.E. Tapiador, Security and privacy issues in implantable medical devices: A comprehensive survey, J. Biomed. Inform. 55 (2015) 272–289, https://doi.org/10.1016/j.jbi.2015.04.007.
[172] Tissue–electronics interfaces: from implantable devices to engineered tissues | Nature Reviews Materials, (n.d.). https://www.nature.com/articles/natrevmats201776 (accessed June 28, 2023).
[173] S.H. Lee, B.H. Kim, C.G. Park, C. Lee, B.Y. Lim, Y.B. Choy, Implantable small device enabled with magnetic actuation for on-demand and pulsatile drug delivery, J. Control. Release 286 (2018) 224–230, https://doi.org/10.1016/j.jconrel.2018.07.037.
[174] H. Liu, T. Zhao, W. Jiang, R. Jia, D. Niu, G. Qiu, L. Fan, X. Li, W. Liu, B. Chen, Y. Shi, L. Yin, B. Lu, Flexible battery-less bioelectronic implants: wireless powering and manipulation by near-infrared light, Adv. Funct. Mater. 25 (2015) 7071–7079, https://doi.org/10.1002/adfm.201502752.